



TECHNISCHE
UNIVERSITÄT
WIEN

DIPLOMARBEIT

Microclimatic conditions and modeling possibilities of the Dachstein-Rieseneishöhle

unter der Anleitung von

Associate Prof. Dipl.-Ing. Dipl.-Ing.(FH) Dr.techn. Matthias Schuß

E 259-3 Abteilung für Bauphysik und Bauökologie
Institut für Architekturwissenschaften

eingrichtet an der

Technischen Universität Wien
Fakultät für Architektur und Raumplanung

von

Zalan Bajka

Matr. Nr.: 1429847



Wien, September 2021

Abstract

The *Dachstein-Rieseneishöhle* is one of the most important caves in Austria that hosts perennial ice. It is an ice cave that is located in the UNESCO world heritage site of *Hallstatt-Dachstein / Salzkammergut* (WHS 806). In Austria, it is considered a natural monument (*nd597*) and a nature protection area in the EU (*AT3101000/EU02*).

Although caves are considered to be a stable climatic environment, protected from the outer extremes by the temperature filtration effect of its properties, the regional temperature trends seem to work against additional ice accumulation and presents a danger of a fastening degradation.

Scientists started to monitor the cave shortly after its exploration in 1910. The latest climatic study started in late 2017. The results between 2018 and 2020 are evaluated and compared to those of the previous decades that were in the archives of the *Karst- und Höhlen-Arbeitsgruppe* in the *Naturhistorisches Museum Wien*.

The results agree with the local climate change prognoses of the Eastern-Alps. There is a clear indication that the mean annual temperature increase outside the cave since 1950 is strongly correlated to the simulations that predict the climate of the 21st century in the region.

This resulted in a significant temperature change in the cave halls, where glaciation happens. They are on average more than two degree Celsius warmer in the cooling period of winter. The same part of the cave is on the edge of the glaciation temperature zone in the summer, whereas it was well below the freezing point in the monitoring period of 1956-1958.

The cave management has some tools that can help to control the glaciation process, in the form of weather doors, that can block the influx of warm air or the outflow of colder cave air depending on the season; however scientists disagree on the magnitude of thermal energy that is transported into caves with the air movement.

Kurzfassung

Die Dachstein-Rieseneishöhle ist eine der bedeutendsten Eishöhlen Österreichs. Die Höhle befindet sich im UNESCO Welterbegebiet Hallstatt-Dachstein / Salzkammergut (WHS806). Sie wurde 1973 zum Naturdenkmal (nd597) erklärt und liegt eingebettet in einem europäischen Naturschutzgebiet (AT3101000/EU02).

Obwohl Eishöhlen ein relativ stabiles Höhlenklima im Vergleich zu den äußeren Wetterbedingungen aufweisen, scheinen die regionalen Temperaturentwicklungen dem üblichen winterlichen Eisaufbau entgegenzuwirken. Dies stellt auf lange Sicht eine erhebliche Gefahr dar und kann zu einer nicht reversiblen Reduktion der Eismassen führen.

Erste wissenschaftliche Aufzeichnungen des Innenklimas der Dachstein-Rieseneishöhle begannen bereits nach ihrer Entdeckung im Jahr 1910. Die neueste seit 2017 laufende Höhlenklimastudie ermöglichte neue Daten aus 2018 bis 2020 mit jenen aus vergangenen Jahrzehnten (dokumentiert im Archiv der Karst- und Höhlen-Arbeitsgruppe des Naturhistorisches Museum Wien) zu vergleichen.

Die Werte des lokalen Außenklimas stimmen gut mit den lokalen Klimawandelprognosen der Ostalpen überein. Es gibt einen klaren Hinweis, dass der Anstieg der mittleren Jahrestemperatur außerhalb der Höhle seit 1950 mit den Temperaturanstiegsvorhersagen der Region korrelieren.

Dies führte auch zu einer erheblichen Temperaturveränderung in den einzelnen Höhlenabschnitten mit entsprechendem Einfluss auf die winterliche Eisbildung. Konkret sind die Durchschnittswerte in den winterlichen Kühlperioden um mehr als zwei Grad Celsius gestiegen. In den Sommerperioden sind jene sogar durchgehend positiv, während diese im Zeitraum von 1956 und 1958 unter dem Gefrierpunkt lagen.

Die Höhlenverwaltung verfügt über einige Instrumente, die für die Eiserhaltung unterstützend sind. Durch Wettertüren und Lüftungsklappen kann speziell in der warmen Jahreszeit die Einströmung von warmer Luft bzw. Ausströmung von kälterer Höhlenluft reduziert werden. Hierdurch ist eine aus Sicht der Wissenschaft begrenzte Beeinflussung der Luftströmungen und folglich des Höhlenklimas möglich.

Acknowledgement

Foremost, I would like to sincerely thank the help and guidance of Associate Prof. Dipl.-Ing. Dipl.-Ing.(FH) Dr.techn. Matthias Schuß, who made it possible to be a part of this monitoring effort.

Furthermore, I would like to express my gratitude to Dipl.-Ing. Dr. techn. Claus Pröglhöf and to the colleagues of the Dachstein Tourismus AG.

I am also grateful to Ing. Dr. Rudolf Pavuza for the opportunity at his department.

I also had great pleasure of studying at the Department of Building Physics and Building Ecology under the leadership of Univ.Prof. Dipl.-Ing. Dr.techn. Ardeshir Mahdavi and I am especially thankful for the classes of Univ.Assistant Dipl.-Ing. Dr.techn. Ulrich Pont.

Finally, I would like to thank Flóra her unwavering support and patience that cannot be underestimated!

Contents

Contents	IV
List of Figures	VI
List of Figures	VII
List of Tables	VIII
List of Tables	VIII
List of Abbreviations	IX
1 Introduction	1
1.1 Motivation	2
1.2 Objective	2
2 Background	4
2.1 Speleology	4
2.2 Ice caves	5
2.3 Geographical context	12
3 Historical overview	16
3.1 Exploration of the cave	16
3.2 Surveys	20
3.3 Speleoclimatic observations	21
4 Methodology	25
4.1 Analysis of the literature	25
4.2 Data collection	25
4.3 Data quality	29
5 Results of the monitoring	31
5.1 Cave climate regimes	31
5.2 Trends in the region	32
5.3 Annual trends	39

6	Ice cave models	44
6.1	First approaches	44
6.2	Mass and energy balance	45
6.3	Cave airflow models	49
7	Conclusion and Outlook	55
7.1	Future research	56
	References	58
	Bibliography	58
	Appendix	61

List of Figures

2.1	Ice cave classification by Luetscher.	9
2.2	Temperature distribution in karsts.	10
2.3	Main factors of the cave microclimate depicted as speleophysiology.	11
2.4	Map of the Alps.	12
2.5	Map of the Dachstein region.	13
2.6	Snow volume changes in relation to the altitude.	15
3.1	Map of the Dachstein-Rieseneishöhle from 1913.	18
3.2	Comparison of different Dachstein-Rieseneishöhle depictions.	22
4.1	Original notes from Saar.	27
4.2	Location of the weather stations.	28
5.1	Air flow direction and velocity in the cave.	32
5.2	Mean air temperature in the different regimes at the current measuring stations.	33
5.3	Mean monthly air temperature in the transitional period.	33
5.4	Mean air temperature in the winter and summer regimes.	34
5.5	Cumulative distributions of T at the station SCH and KRP.	35
5.6	Standard deviation of the measurements at SCH and KRP.	36
5.7	Mean temperature differences of SCH and KRP.	36
5.8	Mean annual air temperatures aggregated by the summer and winter regimes.	37
5.9	Annual precipitation in the different regimes.	37
5.10	Annual snowfall measurements at the SCH and KRP stations.	38
5.11	Snowfall minima and maxima with monthly distribution.	38
5.12	Mean monthly air temperature in the <i>Parsivaldom</i>	40
5.13	Mean annual air temperatures grouped by the observation periods.	41
5.14	Air temperature in relation to distance into the cave.	42
5.15	Mean temperatures aggregated by the summer and winter regimes in the period of 2018-2020 and compared to the station distance from the cave entrance.	43

6.1	Chronology of the ice cave theories.	45
6.2	Air flow velocity in the <i>Tristandom</i>	51
6.3	Explanation of the cave pressure gradient differences.	52
6.4	Hydrostatic pressure model.	53
7.1	Map of the Dachstein-Rieseneishöhle by Saar	62
7.2	Sections of the Dachstein-Rieseneishöhle by Saar	64
7.3	Heatmap of Schönbergalm and Krippenstein	65
7.4	Overview of the available temperature data	66

List of Tables

2.1	Regulating factors of cave glaciation	8
4.1	Weather stations at the <i>Schönbergalm</i> and <i>Krippenstein</i>	26
4.2	Current and past monitoring locations.	28
4.3	Locations of the online weather stations.	30
5.1	Frost days in the <i>Parsivaldom</i> (at MS 10)	41
7.1	Rock temperature measurements by Saar in 1928-29.	63
7.2	$\Delta T = T_{measurement} - T_{virtual}$	67
7.3	$T_{virtual}$	68
7.4	Mean daily temperatures in 1928-29 by Saar.	69
7.5	Daily max and min temperatures in 1928-29 by Saar.	70
7.6	Daily mean temperature measurements by Saar 1920-22.	71
7.7	Monthly mean temperatures by Saar from the 1920-24 period.	72

List of Abbreviations

DRE	Dachstein-Rieseneishöhle
DAG	Dachstein Tourismus AG
KRP	Krippenstein
MAAT	Mean annual air temperature
MAT	Mean annual temperature
MMAT	Mean monthly air temperature
SCH	Schönbergalm
SD	Standard deviation

Chapter 1

Introduction

One of the great indicators of past climates and changes in the atmospheric conditions are perennial ice caves. On one hand, they serve as local tourist attractions, on the other hand they function as scientific hubs, where climate researchers have been trying to understand the relations between signals of long vanished atmospheric conditions. These high-definition climate data archives of the previous centuries are not common. Therefore ice core samples are of great interest to the scientific community and preserving the ice reserves in these caves are becoming a major environmental issue.

Understanding the micro-climate of caves, which can nurture ice accumulation through centuries, requires plenty of dependable data in various outside conditions. Brute-force modeling methods that might work in a building-science case, are most likely unattainable with the current technologies in a limestone cave.

The present rate of climate change poses a challenge for experts, scientists and institutions, who are working on conserving the accumulated ice mass for the future.

Scientific research has a long tradition in the Alps. Meteorological observations have been logged at different ice caves dating back to the late 19th century. As the anthropogenic influence on the rate of the climate change became more prevalent, the information contained in these frozen archives became more valuable, because most of these sites are also more exposed to extreme weather conditions, than they were in the previous centuries.

1.1 Motivation

The subject of the thesis, the *Dachstein-Rieseneishöhle* has been studied with scientific instruments since its exploration in 1910. Multiple expeditions investigated the cave and its ice-formations for different periods throughout the 20th century. The measurements they collected are of high value to the scientific community. The program that the Dachstein Tourismus AG started presents a unique opportunity to complement the data-collection efforts of the last century with a historical comparison and analysis.

In order to identify differences and similarities between the past and present cave climate digitizing the old archives and observations played a key role.

Valuable information about long-term trends could be gathered from measurements on this timespan. Daily average temperature values with known location inside the cave are available from 1920.

Predicting changes in a complex system, like a perennial ice-cave presents challenges for the existing methods. Statistical models that might help the cave operators to harness the cooling potentials on certain cold days could be improved with a longer dataset.

The *Dachstein-Rieseneishöhle* is one of the most important ice-caves in Austria. Not only a unique asset for the scientific community, but for the local economy as well. It is fortunate that the cave and its history is well documented in the Austrian speleological literature.

1.2 Objective

One of the primary goals of this thesis is to gather and archive all the known historical data regarding the micro-climate of the *Dachstein-Rieseneishöhle*. The findings are presented alongside a general overview of the exploration timeline and surveying efforts. The past trends are then compared to the observations collected by the cave management and the scientific team since 2017. Given the fact, that the measuring methods in the past, especially in the first part of the 20th century, can not be validated and controlled, the focus is on the trends and the relation between the surveyed locations.

The study continues after the comparison by presenting a summary of the existing mathematical models that can be used to describe the ice-balance changes of the *Dachstein-Rieseneishöhle*. Some of these models require inputs that had not been collected by the scientific team, and therefore they can not be fully implemented.

On the other hand, they provide useful information about the potential expansion of the research.

It is major element of the observation effort that the cave operation will incorporate and utilize the measured data with the aim of reducing the external thermal impacts on the ice-mass-balance of the locations where glaciation occurs. This would be used to provide a better schedule for the available equipment for the purpose of regulating the incoming or outgoing air flow as much as possible.

Chapter 2

Background

The term ice cave is generally understood to mean caves that host perennial ice accumulations; although the scientific community has differing views on the current terminology. This chapter covers the primary nomenclature of the fields focusing on ice caves. Starting from the general cave exploration to the Eastern Alps, where the *Dachstein* mountain is located.

It also provides a brief overview of the scientific disciplines, terminology and some core concepts of the ice cave research. In the later sections, the geographical context of the *Dachstein-Rieseneishöhle* is outlined.

2.1 Speleology

In the late 19th century the science of caves, cave formations and features became a distinct discipline thanks to the work of a Frenchman, Édouard-Alfred Martel (1859-1938). He is considered to be the “father of modern speleology”. In 1895, he founded the first organization that focused on cave science, the *Société de Spéléologie*. Previously the study of caves was part of other larger disciplines such as geology and geography.

In 1952 G. W. Moore introduced the term *speleothem*, which is used to describe secondary mineral cave formations. They are examined extensively as climate proxies, due to their unique environment. Multiple indicators, such as oxygen and carbon isotopes can serve as information sources about temperature and precipitation levels of the past. These deposits provide a very precise dating opportunity for scientists, using uranium-thorium dating method.

A rather new field that grew out of the latter is the *speleophysiology*, introduced by Fairchild et al. (2006). It studies the cave environment as a complex unit; its energy

and mass flows, the functions of ice-accumulation concepts and the cave climate as a whole.

The term “speleothem incubator” is used to describe the circumstances that ensue in a cave, where they contribute to the growth of various mineral formations. The thermal environment is much less dynamic in caves than above the ground, but these small changes in the air temperature, humidity and pressure can determine the rate of the ice and speleothem buildup (Fairchild et al., 2012).

2.2 Ice caves

The terminology to define subsurface ice formations and the caves that host them is often misunderstood and is a victim of influences of the regional vocabulary. Balch (1900) argued that the English term *ice cave* is misleading, because it indicates the type of the geological formation only after its content. He proposed the usage of the French term *Glacière* instead, but the scientific community continued to use the common ice cave label concurrently.

On the First International Workshop on Ice Caves (*Căpuș*, Romania, 2004) the following definition was presented: “ice caves are rock-hosted caves containing perennial ice or snow, or both”. (Luetscher & Jeannin, 2004a)

Exploration of ice caves

In the scientific literature, prior to the 20th century, reports and descriptions about the phenomena dominate. According to Meyer, the first mention of ice caves dates back to the 12th century in Kashmir. Frozen water during the summer in caves located in the Carpathian region is mentioned in 1490 by Petrus Ranzanus (Balch, 1900).

More detailed descriptions origin from the French Alps in the 16th century. Two reports are mentioned in the literature of the late 19th century about the *Chaux-les-Passavant* by the Frenchmen, Poissenot and Gollut (Fugger, 1893).

In the 17th century, ice caves were reported in Slovenia and Slovakia (Fugger, 1893). The first russian literature about an ice cave in the Volga valley appeared in 1690 and was followed by many in the 18th century (Turri et al., 2009).

The research methods regarding the ice caves changed in the late 19th century, becoming more measurement-oriented. Before that era, the explorers mainly focused on discovering and describing the caves themselves, such as Fugger (1891) and Balch (1900), who collected and evaluated historical data in the scientific literature about ice caves. They wanted to have a better understanding where and under what

circumstances these conditions occur that facilitate ice glaciation and maintain the ice mass in summer.

In the early 20th century, Bock et al. (1913) published their findings about the recently discovered *Dachstein-Rieseneishöhle*. They were able to make temperature, air humidity and wind speed measurements to establish a model that could describe the energy intake of the cave. This was the first publication which used a comprehensive physical model to describe the perennial ice accumulation in non-permafrost regions. Although it was a groundbreaking work, for decades it had not been widely discovered in the scientific community.

Distribution of ice caves

Most known cave ice glaciation happens in North America and Eurasia, as it is indicated by the distribution of ice caves around the world (Karakostanoglou, 1989). The boundary conditions for ice accumulation in caves have not yet been clearly defined. There have been multiple studies conducted regarding this question, especially in Russia and in the former USSR, where it was of strategic importance to find locations for ice deposits that do not need artificial cooling.

As quoted and translated by Turri et al. (2009), the Russian researcher Yu. Listov published in 1895 a list of 8 conditions that lead to cave glaciation:

- (I) *Caves have to be situated in the massif of the rocks rising high above the surrounding place.*
- (II) *The rocks have to be sedimentary, of the chemical origin: there are gyphs, limestone, and dolomite.*
- (III) *The rocks have to possess the all-physical and chemical properties, promoting dissolution and washing out by the water: generally, weather easily.*
- (IV) *The rocks have to be the poor conductor of the heat, but in the same time to be possessed the considerable heat capacity.*
- (V) *Air canals and emptinesses, causing the formation of air draught "+" and "-", have to exist in the massif of the rocks.*
- (VI) *The average annual temperature of the area can change from 0 °C to 10 °C, the temperature of July have to be high, but of January, the most cold month of the year, below 0 °C. The hotter is the summer and the more cold the winter, the lower will be the temperature in the ice caves.*

- (VII) *Mountain massif has to be subjected to the all-meteorologic elements.*
- (VIII) *In summer, the ice caves have to be safeguarded against the wind blowing in the entrances.*

(Turri et al., 2009, p. 161)

According to newer research, the mean annual air temperature (MAAT) in the Eurasian regions where we can find perennial cave ice, is indeed between 0 °C and 10 °C, just as Listov argued. There are exceptions with below 0 °C MAAT areas. These values do not define any clear boundary conditions, only illustrate the statistical data that were mostly collected in almost 80 caves in the former USSR (Karakostanoglou, 1989). The classification efforts showed, that concentrating only on the altitude and the latitudinal location of the cave could not determine any zones, only lead to the aforementioned boundary values.

Malyudov (1989) describes a list of prerequisites for cave glaciation: (I) outside climate, (II) cave microclimate and (III) hydrology.

- (I) The outside air temperature must be below 0 °C at least in a part of the year.
- (II) If the cave is not located in the permafrost zone, then there must be an adequate cave formation that enables a frosty air inflow alongside an existing cold substance accumulation.
- (III) The cave has to have a water source (in any state).

If the prerequisites are met, (A) the right combination of external and cave temperature, (B) the cave form, (C) the amount of cold storage and (D) the water inflow regulates the glaciation.

- (A) The ratio, the *cave glaciation index*, is characterized by the K value (it is also called *CGI*). This is an approximation, that is validated with data analysis on caves in the former USSR.

$$K = \frac{-T_{cm}}{T_{cave} - T_{cm}} \quad (2.1)$$

Table 2.1: Relations of the regulating factors of the cave glaciation.

water input	cave air temperature	cold content	ice content
c	↓	↑	↑
↑	↓	↑	↑
↓	↓	↑	↓
↑	c	c	↑
↓	c	c	↓
c	↑	↓	c
↑	↑	↓	↑
↓	↑	↓	↓

C - constant; ↑ - increase; ↓ - decrease. *Notes.* Adapted from “Cave glaciation”, Malyudov, 1989, p. 299.

Classification of ice caves

According to studies of caves in temperate regions, two types of ice caves can be distinguished based on cave air dynamics. The ice formation in a static ice cave stems from thermal trapping, that forms a *cold air trap*. In a dynamic ice cave, depending on the geometry and location, barometric and convective circulation lead to glaciation. Additionally, one can use a different system that is based on the origin of the cave ice.

Thury argues (as cited by Meyer (2018)), that the winter season is the most relevant in static ice caves regarding the ice accumulation. He uses the term *open period* because the temperature and density differences between the cave and the outside air cause circulations that are not present in the summer. Luetscher and Jeannin (2004a) mention that although the summer period is not the determinant, natural convection is demonstrably present, but plays a significantly lesser role in the energy balance of the caves.

In an ideal dynamic ice cave the *chimney effect* is mostly responsible for the ice glaciation. It occurs when the cave has two or more entrances at different elevations. The pressure, density, and temperature differences between the outside and the cave air causes the circulation. These flows are unidirectional in nature and since the cave temperature is close to constant during the whole year, the direction changes according to the season. In the winter period, cold air flows in at the lower entrance. The reality is, of course, much more nuanced and such simplifications are not correct. Especially in a karst environment with various types of thermal energy exchanges occurring simultaneously. Barometric and convective air circulations have secondary effects with secondary, smaller air flows in different directions depending on the cave geometries.

As there are caves that can be referred to as both static and dynamic, a new term, *statodynamic* ice cave was later added to the terminology.

As figure 2.1 illustrates, Luetscher and Jeannin (2004a) suggested a combined classification system that unites the CAD-based method with the origin-based one. This method includes more geological information than the other two.

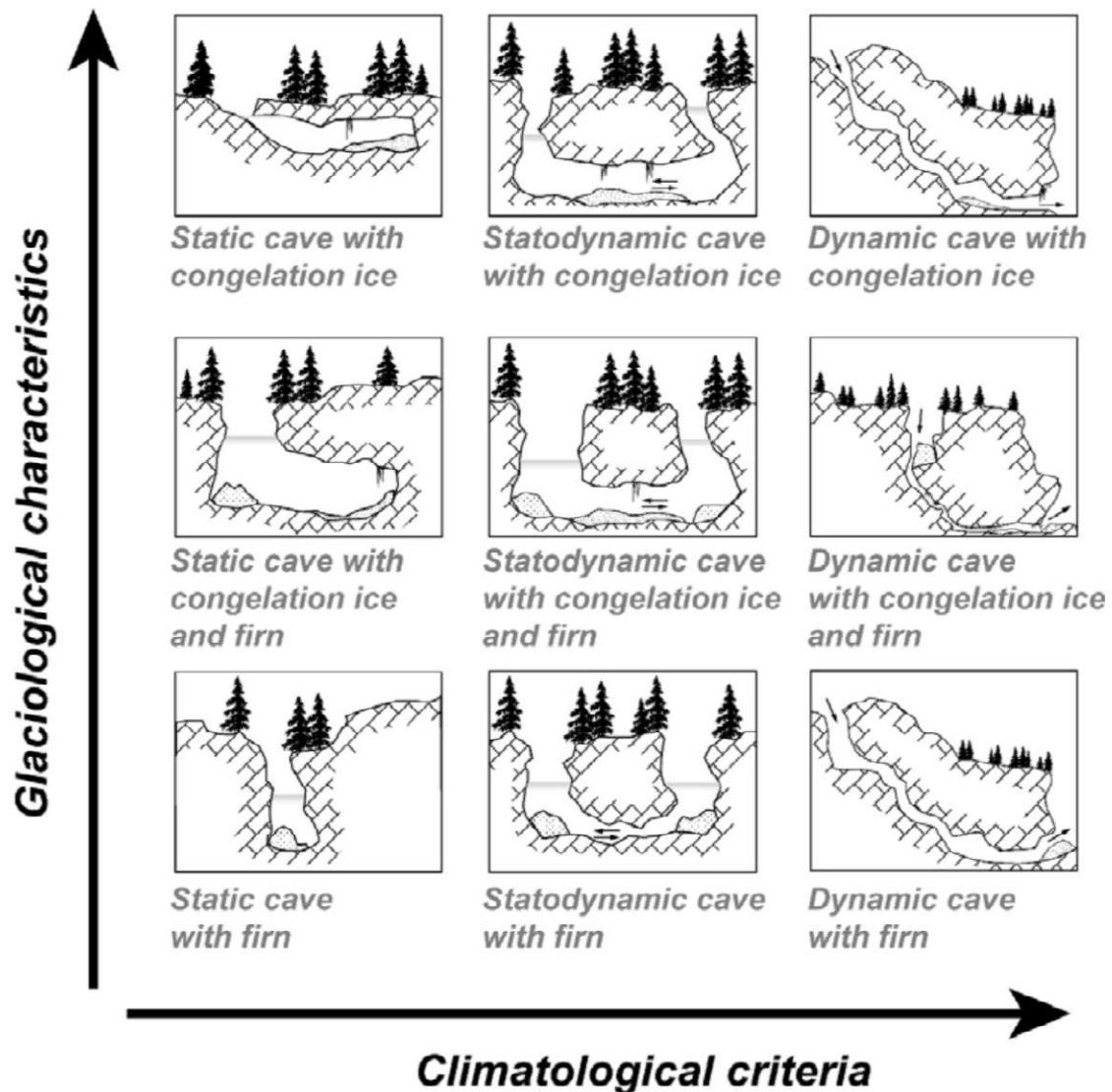


Figure 2.1: Ice cave classification suggested by Luetscher. *Notes.* Reprinted from “A process-based classification of alpine ice caves”, Luetscher and Jeannin, 2004a, p. 8.

Energy inputs of caves

Although mean monthly cave temperatures are known to be mostly constant throughout the different seasons, the governing energy balance is rather complex. There are multiple major and minor factors that affect the inside air and surface

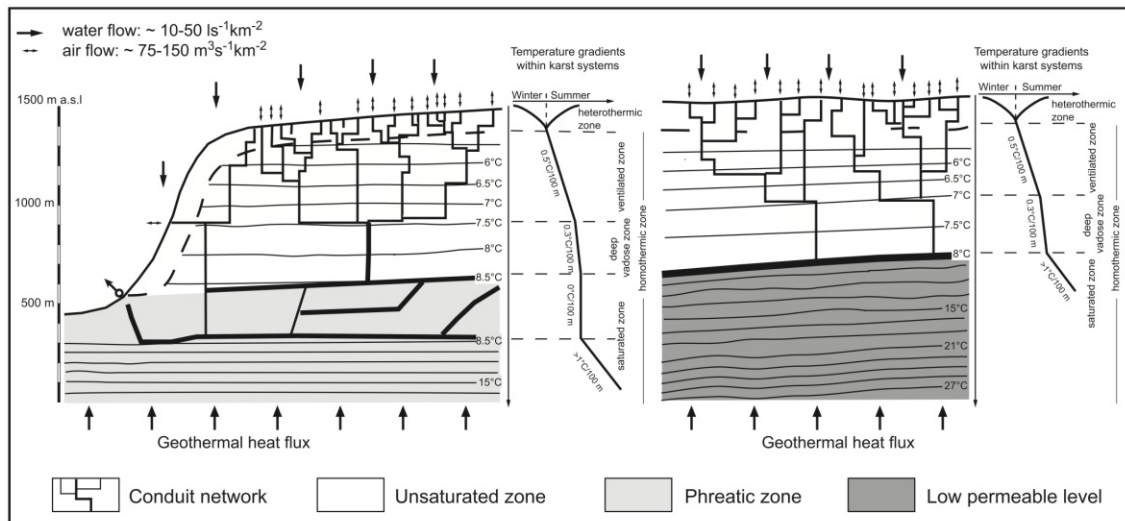


Figure 2.2: Temperature distribution in karsts. *Notes.* Reprinted from “Temperature distribution in karst systems: The role of air and water fluxes”, Luetscher and Jeannin, 2004c, p. 345.

temperature. The significance of these factors shows great variety in different cave types.

As illustrated by Luetscher and Jeannin (2004c), Fig. 2.2 demonstrates how cave energy inputs are linked to the cave depth. The zone closest to the entrance, called the *heterothermic zone*, is still heavily influenced by the outer climate. Depending on the cave ventilation, this can be at least 50 m deep. The conduits, where the temperature does not show strong seasonal variations, are called the *homothermic zone*. In the heterothermic zone, the karst is not fully saturated with water (vadose zone). The homothermic zone can be further divided into groups based on the saturation level of the surrounding rocks: (I) the ventilated zone, where the air circulation is still relevant, (II) the deep vadose zone and (III) the saturated zone, where the horizontal temperature gradient is close to zero.

The main heat sources of thermal energy in a cave are on one hand the heat transferred from the inner core of the planet and on the other hand the heat from the atmosphere. Advection and conduction are the most dominant sources of heat exchange. The high level of humidity in the cave environments has a significant effect on the overall energy balance due to evaporation and condensation. Heat can be transferred and stored as sensible or latent heat. Sensible heat occurs through a change of temperature, whereas latent heat is the energy that is needed for a phase change. Evaporation and condensation mean that the energy is not transformed as temperature change, but as isothermal phase change.

The geothermal heat flux is calculated by temperature profiles that are measured in deep caves and mines. Where the subsurface water flows are not significant, the

(a)

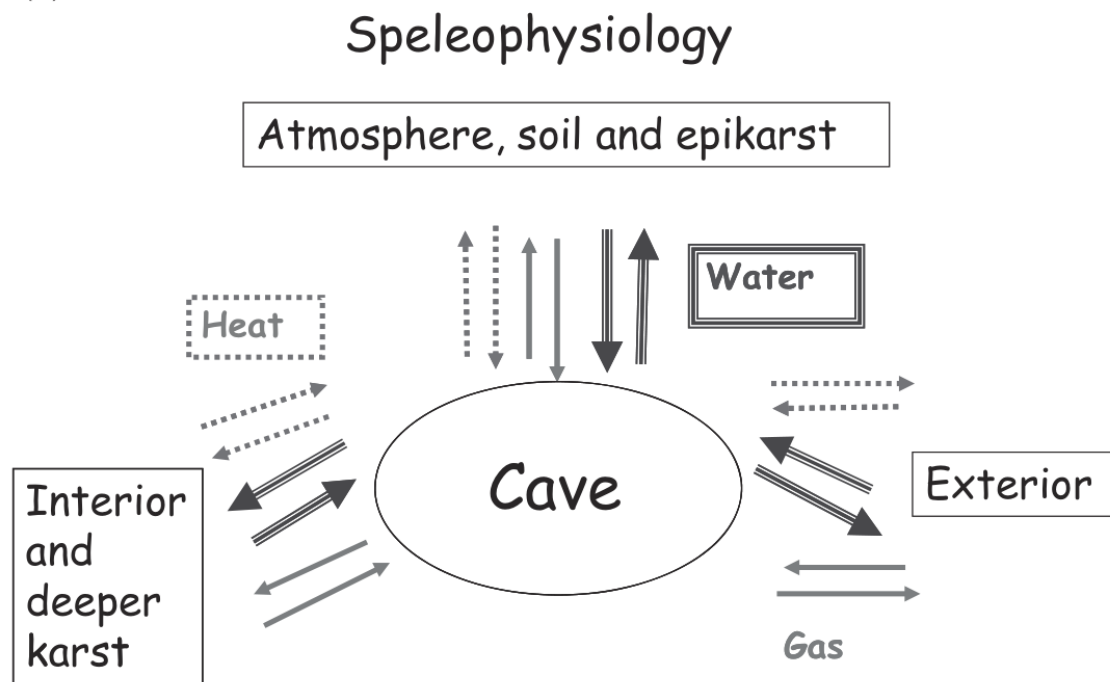


Figure 2.3: The main factors of the cave microclimate depicted as speleophysiology. *Notes.* Reprinted from *Speleothem Science: From Process to Past Environments*, Fairchild et al., 2012, p. 108.

temperature increases with a constant rate. It is called the *geothermal gradient*, which lies usually in the 1.8-3.5 °C/100m region.

The heat transferred by the atmosphere is the most significant in the heterothermic zone. In case the internal and the external air humidity and temperature are known factors, the position inside the cave - where the external and the internal cave temperature is in equilibrium - can be calculated with the following equations (Wigley & Brown, 1971) :

$$T = T_a + (T_0 - T_a) e^{-X} + \frac{L}{c} (q_0 - q_a) X e^{-X} \quad (2.2)$$

$$(1 + A) \ln \left[\frac{T_1 - T_a}{T - T_a} \right] + AB (T_1 - T) = X - X_s \quad (2.3)$$

In most caves where the water or air advection is not especially significant, the rock temperature determines the overall cave temperature, due to the large thermal inertia of the material. In this case, most of the thermal exchanges occur in the form of conduction. The value of $10^{-6} \text{ m}^2 \text{ s}^{-1}$ is commonly used for rock diffusivity in thermal propagation calculations (Fairchild et al., 2012).

2.3 Geographical context

This section looks at the geographical location of the *Dachstein-Rieseneishöhle* and the challenges in the region due to the increasing rate of the environmental and climatic changes.

Dachstein

The *Dachstein* mountain range is part of the Northern Limestone Alps according to the Alpine Club classification of the Eastern Alps (*Alpenvereinseinteilung der Ostalpen, AVE*) (see Figure 2.4). The range includes the *Dachstein* massif with the *Hoher Dachstein*, the *Grimming* and *Sarstein*. The *Hoher Dachstein* is often called the “three-state mountain” (*Drei-Länder-Berg*) as it is situated in three different *Bundesländer* (*Oberösterreich*, *Steiermark*, and *Salzburg*). Its highest peak is at 2,995 m and has a topographic isolation of around 47,7 km. The formation of the limestone started in the Triassic times. Being predominantly karstic, the massif is permeated with numerous caves. Besides the *Dachstein-Rieseneishöhle*, there are two other significant caves nearby. The *Eisriesenwelt* (one of the biggest ice caves of the world with the largest known ice surface) and the *Mammuthöhle* (situated next to the *Dachstein-Rieseneishöhle*). There are three large glaciers on the mountain, the *Hallstätter Gletscher*, the *Großer Gosaugletscher* and the *Schladminger Gletscher*, but unfortunately, they appear to be retreating steadily.

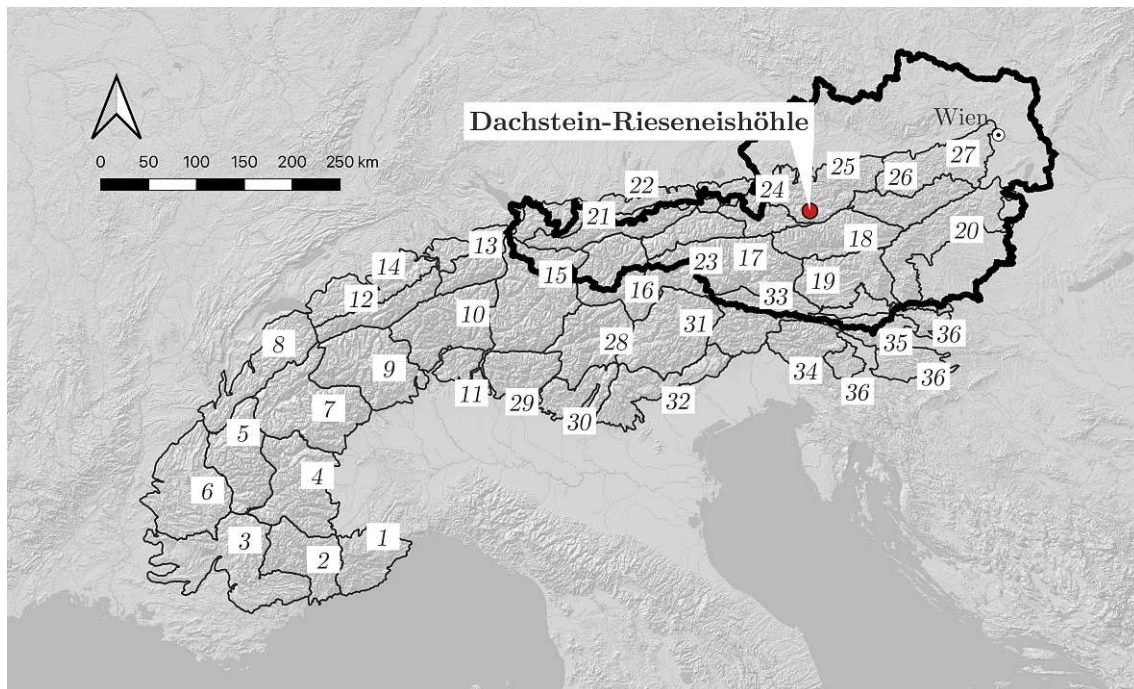


Figure 2.4: Map of the Alps with the *SOIUSA* classification system.

Dachstein-Rieseneishöhle

The *Dachstein-Rieseneishöhle* is one of the biggest ice caves in Europe. It is located on the northern side of the *Dachsteinmassiv*. Since its opening in 1912, it has become an important tourist attraction in the *Obertraum* area. The entrance is situated at 1420 m.ü.A. on the *Schönbergwand*. The surface area of the cave is close to $5000m^2$, while the approximated ice mass is around $13000m^3$. The current explored length is about 2700 m and the height difference is close to 90 m. According to Schmeidl (1969), the pollenanalysis shows that the oldest ice layers in the cave are about 500-600 years old, while the top layers are not older than about 100 years. Some of the famous ice monuments are also relatively young, i.e., the *Monte Cristallo* is dated back only a few dozen years.

According to the standard classification, the *Dachstein-Rieseneishöhle* is regarded as a dynamic ice cave. It has multiple air-flow streams and depending on the season, the main direction of the circulation changes.

Since 1973 it is part of the UNESCO world heritage site of *Kulturlandschaft Hallstatt–Dachstein/Salzkammergut* (WHS 806).

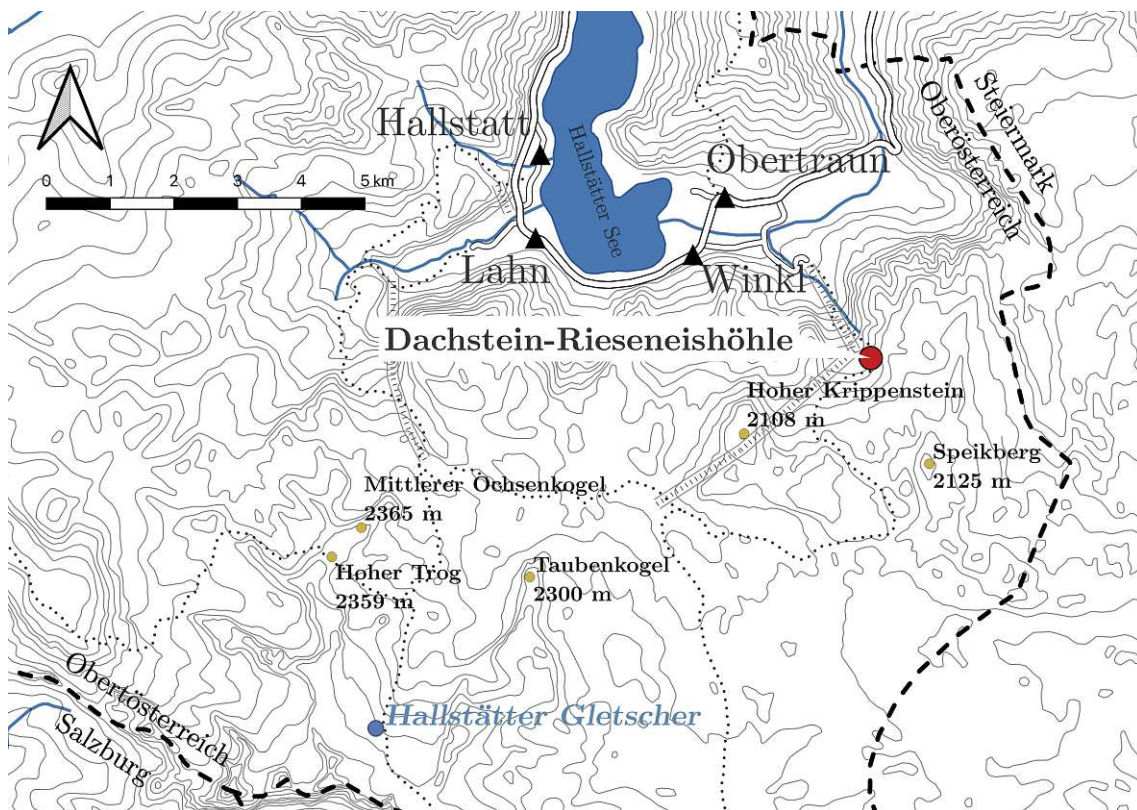


Figure 2.5: Map of the Dachstein region with the neighboring peaks and towns.

Climate change in the Alps

The consequences of the rapid climate change are especially significant in the alpine regions. The overall temperature increase in the Alps is much higher compared to the European average. The rising temperature changes the hydrological cycle as well inducing an increased rate of evaporation and faster ice melting. A significant decrease of the snow cover in the lower altitudes is also expected by the climate models (Holzmann & Koboltschnig, 2010).

The current trend predicts that the water regime in higher mountains will change fundamentally. According to recent studies, more than half of the alpine glaciers will disappear until the year 2050. The guaranteed snowfall altitude will also change drastically and rise about 200-400 m by the end of the 21th century. It is expected not to see snow below the 1000 m altitude (see Figure 2.6).

Although ongoing permafrost degradation causes an increased debris flow rate on the mountain slopes that might have a positive feedback-loop; other factors could have a much higher impact than the current models suggest. The precipitation in the Alps during the winter season will most definitely increase and decrease during the summer season. It indicates that a recurring drought season can be anticipated, especially in the southern regions of the Alps (Gobiet et al., 2014).

The energy balance of an ice cave is complex. Some factors of the climate change might seem to benefit the perennial ice (less water flow in the summer season), but the overall energy surplus that comes with the increased atmospheric temperature will slowly make the ice disappear in caves which are located on a lower altitude.

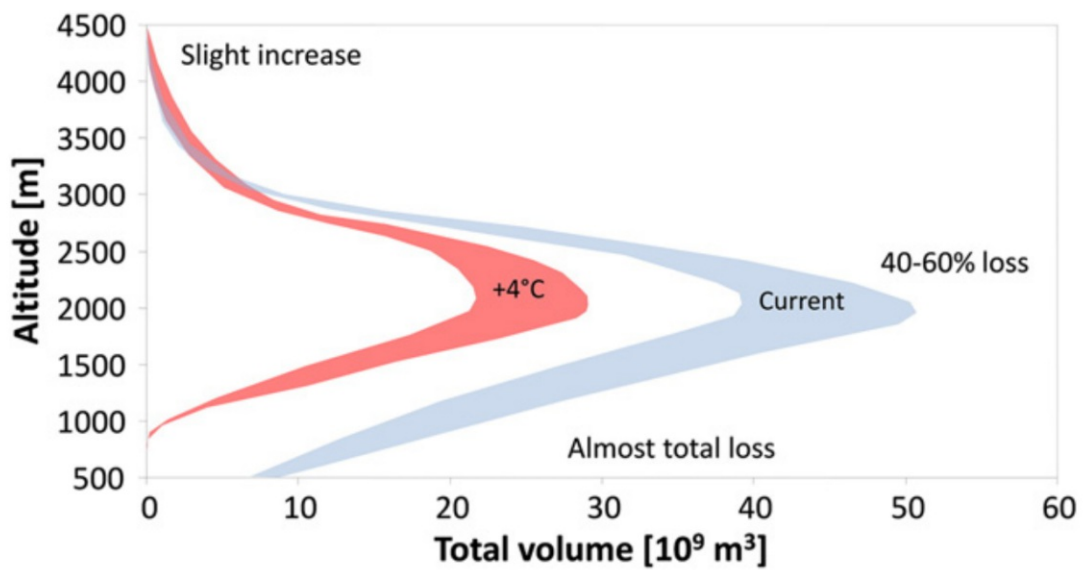


Figure 2.6: Snow volume changes in relation to the altitude. The occurrence of snow below 1000m is not anticipated according to the predicted models (calculated with an average of +4°C temperature change in the region). *Notes.* Reprinted from “21st century climate change in the European Alps - A review”, Gobiet et al., 2014, p. 1147.

Chapter 3

Historical overview

Although many caves of the *Dachstein* region had been already known to the locals, the presence of permanent ice was first mentioned in the scientific literature in the late 19th century. The *Dachstein-Rieseneishöhle* was explored in 1910 by Georg Lahner. This chapter covers a brief timeline of the cave expeditions, the cartographical surveying and the scientific data collecting efforts. As the older literature was published almost exclusively in German, the aim of this section is to present a comprehensive picture for a wider English speaking community.

The information used in the study was gathered mainly from the publications of famous Austrian cave explorers, speleologists and engineers, such as G. Lahner, H. Bock, G. Kyrle and R. Saar.

3.1 Exploration of the cave

The first written mention of the *Dachstein-Rieseneishöhle* was made by Dr. Robert J. Arnold in the *Steierischen Alpenpost* (Nr. 36, 1910). According to his report, the entrance of the cave was discovered in 1897 by a local shepherd, Peter Gamsjäger. However, it is more likely that the location had been already known to the residents, he was the first one to find a route going deeper into the mountain, as he was looking for a strayaway cattle. Without the necessary equipment and knowledge, he was not able to explore the cave furthermore, but he used his findings to create a local tourist attraction.

In 1908 Alexander Mörk von Mörkenstein, a speleologist from Salzburg and Prof. Witte explored a further 50 m of the cave, interestingly not at the same time. They discovered an enormous hall with a 25 m deep shaft. They could not carry on with the exploration, due to the lack of serious caving equipment, however they made the first measurements in the so-called *Großen Eisabgrund*.

The official discovery date of the ice cave is the year of 1910. Georg Lahner, the speleologist from Linz, was the first one to organize a scientific exploration into the *Dachstein-Rieseneishöhle*. While preparations for the mission were underway, he hired his fellow Linzer Josef Kling to conduct the reconnaissance works of the cave entrance. It is important to mention that they made the first known photograph of the cave in the same year.

On the 17th of July, 1910, Lahner conducted the first scientific exploration of the cave, accompanied by Kling, Ing. Julius Pollak from Wels and a small group of auxiliaries. They were equipped with proper caving equipment and tools. The cave had a narrow and very cramped path right from the opening, caused by some collapsed rocks, that could only be taken in a crouched position. It took 30 m after the narrowing to reach the spacious hall that had already been previously described by Mörk and Witte. They named the section the *Tristandom*. The ceiling reaches more than 10 m above the ground level, while the shaft is around 25 m deep. The group could reach the bottom only with the help of a rope ladder. Lahner reports gargantuan ice blocks and vertical walls all around. They could not go any further as no way was found circumnavigating the shaft. Pollak started to map the explored area right away, while Kling made the first photographs of the inner parts with the help of some magnesium flashlights.

On the 21th of August, 1910, Lahner returned with the chief of the Austrian caving association (*Verein für Höhlenkunde*), Ing. Hermann Bock from Graz and his wife, Hanna Bock. With the expertise of Bock, they could pass the shaft alongside the ice walls and continued exploring the deeper parts of the cave. It became obvious that a much larger expedition group is needed for further investigations. Lahner and Bock immediately started to gather resources for the next trip. Julius Wimmer, the president of the *Sparkasse Linz*, covered the expenses. Many researchers tried to join the caving association, just to be part of the new sensation.

The next expedition that was undertaken on the 11th of September, 1910, was organized by Lahner and Bock. The participants were Hanna Bock, Josef Kling, Alexander Mörk von Mörkenstein, Rolf Saar, Dr. Alois Hobelsperger, Leopold Potisek, Johann Klimek and Lajos Kraul with the help of a small auxiliary group. Initially, they planned for a longer journey, with enough food and equipment for up to 48 hours. The group could pass through the *Tristandom* using the large amount of rope ladders that they brought with.

Right next to the *Tristandom* lies a huge, 8 m high and around 15 m wide stalagmite formation, called the *Monte Cristallo*. They continued eastbound, where an ice stream, the *Kristallo-Gletscher* descends with a maximum of 40° gradient for around

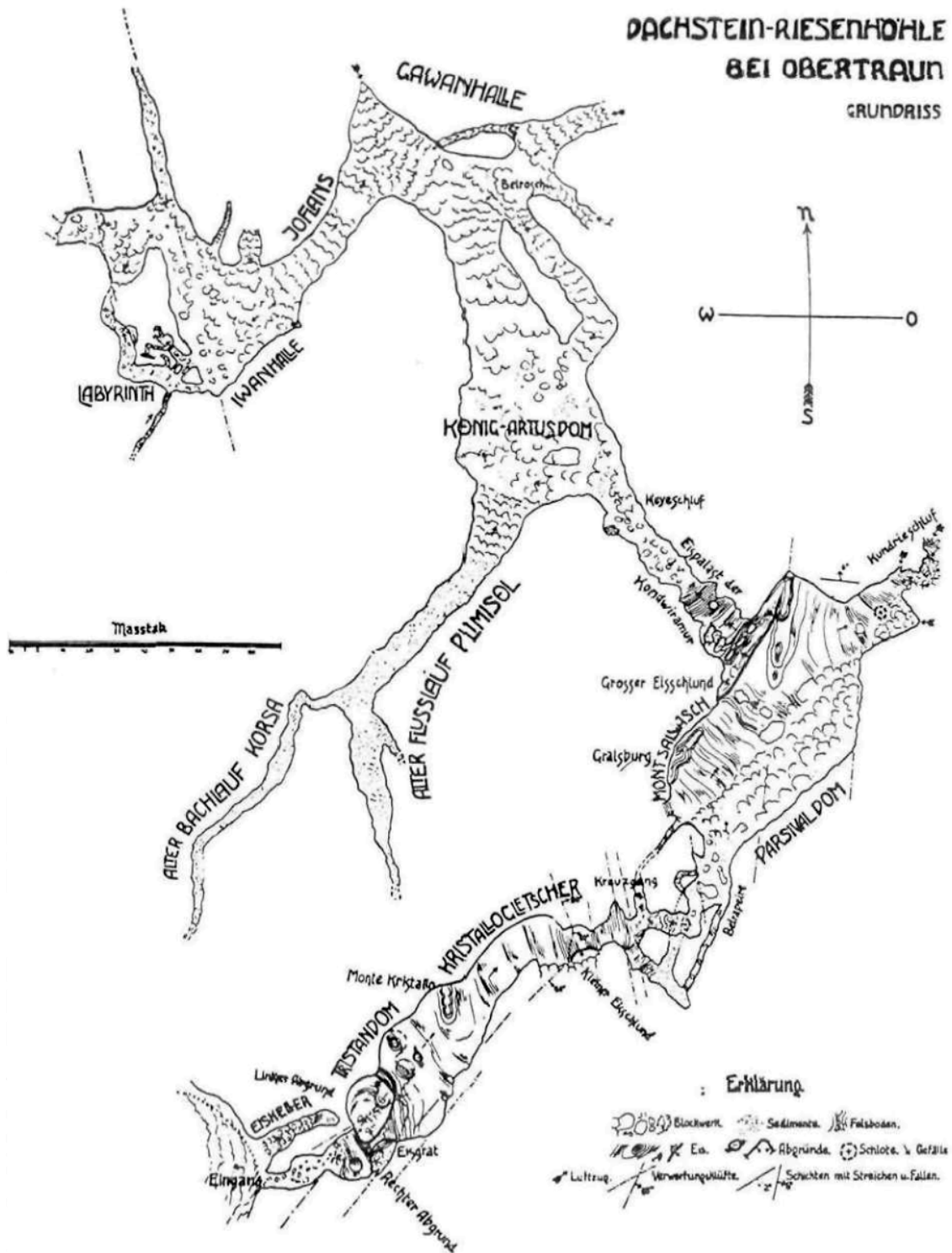


Figure 3.1: Map of the Dachstein-Rieseneishöhle from 1913. Notes. Reprinted from *Höhlen im Dachstein und ihre Bedeutung für die Geologie, Karsthydrographie und die Theorien über die Entstehung des Höhleneises*, Bock et al., 1913, p. 22.

a 100 m. According to Bock, the surface of the ice was so rough in this section that they were able to cross it without any safety equipment. Then they reached a deep ice chasm, the *Kreuzgang*.

This area is surrounded by nearly vertical walls that lead to an ice-free passage, called the *Belrapiere* (named after a city in the *Parzival* saga). Remarkably, the first fossils were found here, i.e. a tooth of a cavebear (*Ursus Speleaeus*).

As they managed to overcome the walls, they entered a gigantic hall, the *Parsivaldom*. It is estimated to be roughly 100 m long, 50 m wide and 25 m high. On the north-western side, a huge amount of ice streams downward forming various ice structures, called the *Montsalvachgletscher*. Some of the formations hang from the ceiling, others grow from the ground, caused by the warmer seepage water flowing down through the cracks. Some fallen rocks on the north-western part of the hall formed a small (only 1 m high) passage that Bock found and later named *Keyeschluf*. After a cramped crawl, he had a glimpse of an even greater hall.

After the whole team passed the *Keyeschluf*, they started to explore this vast formation, the *König Artusdom*. Bock and Lahner began mapping the *Artusdom* outright. They discovered a huge extension on the north side, the *Gawanhalle*. These two halls together are around 200 m long, and 30-60 m wide. At its largest section, the *König Artusdom* is 30 m high.

West from the *Gawanhalle*, the team found an obstructed air shaft. The *Joflans*, a large plateau that leads southwest from the shaft, joins a similar space in size, the *Iwanhalle*. Some smaller extensions south of the hall are called the *Labyrinth*. The ground surface is covered with very loose and fragmented stone shards. The *Iwanhalle* is 70 m long and 40 m wide, but only 10 m high, being smaller than the neighboring *Artusdom*.

On the eastern side of the *Artusdom*, a steep way on the rocks leads to a passable tunnel that is situated ca. 30 m higher than the floor level of the *Artusdom*. It is spacious, covered with deposit rocks and has signs of erosion on the walls. This gave enough evidence for the explorers to assert that they see some ancient watercourses that most definitely helped to carve out the newly discovered cave formations. For the name of this tunnel they reached back again to the *Parcivalsaga* and called it the *Flußlauf Plimisoel*.

After 70 m, a smaller route opens up on the right side, where some tall clay formations were found. This tunnel consists of the same stones and wall erosions as the *Plimisoel*. The group reached a point, where the clay piles were so dense, that they were unable to pass. They called this section the *Bachlauf Korsa*, which

was then later connected to the outside and has been used as the entrance since 1952. This was the last part of the cave that the expedition discovered that day. They found their way back without any accident and reached *Obertraun* in the morning of 12th. Dr. Rudolf Saar and Dr. Alois Hobelsperger performed the first stress tests in the cave in September of 1910.

The next discovery took place on the 4th of September, 1911, after Bock examined the preparatory works in the cave for the upcoming Speleologists Congress (*Speläologen-Kongreß*). Due to the findings in the *Dachstein-Rieseneishöhle* the previous year, the congress was held in *Hallstatt* (the first time in Austria). Bock located a new passage in the southern part of the *Parsivaldom* that leads to a 20 m wide, 30 m long and around 15 m high room, which is situated about 50 m under the ground level of the neighboring *Belrapiere*. He named it the *Anfortashalle*.

After the 17th of July in 1912 the cave was opened for the first time as a tourist attraction in the organization of the *Verein für Höhlenkunde in Österreich* with almost 500 visitors in the first year.

3.2 Surveys

The mapping of the cave had already been started right after the first expedition in 1910. In the course of the *Höhlenforscherwoche* of 1910, a mission that lasted 27 hours, could document almost 2 km of the cave. Figure 3.1 illustrates the first comprehensive map of the *Dachstein-Rieseneishöhle* published by Bock in 1913, that was based on the reports of the mission during the *Höhlenforscherwoche* of 1910. The next significant step in the documentation of the cave was the map of Saar in 1921, as it was regarded as the definitive map in the following decades.

In 1930, the *Österreichischen Bundesforste* ordered a theodolite survey (conducted by Ing. Potuschak) due to the upcoming construction works in preparation for a circular pathway (although it was finished only decades later, in 1951). This survey and the existing documents of Bock were the basis of the mapping project of 1953, created by B. Wagner.

In 1991, a team of professional surveyors and cave cartographers constructed a new ground plan with contemporary technology (digital point-clouds, three-dimensional model).

Comparing the different maps of the various authors shows that the first survey of Bock was already fairly accurate. The connections of the various spaces were well documented (see Fig. 3.2). The surface details are also in line with the survey of 1991. The map published by Saar in 1921 confirmed the drawings of Bock, but also

extended them with isolines for a more precise height representation. The map of Wagner makes references to the surfaces of the cave. He also used the theodolite survey of Potuschak, but for unknown reasons the isolines are not portrayed, which can be considered a step-back from the map of Saar. The map of Seemann from 1999 is the most precise one that is regarded as the chart of the cave until this day.

3.3 Speleoclimatic observations

The phenomena of ice being present in caves during the summer season has been known for a long time in the Alpine regions, but the scientific investigations about this subject date back only to the 18th century. The earliest scientific literature in Austria about ice cave climate observation is a report from F.A. Braune about the *Großen Eiskeller* that was published in 1802. In 1846, Friedrich Simony started climatic observations in the *Dachstein* region and later disclosed his study of the *Gschlösslkirsche* in his main work (*Das Dachsteingebiet*, 1895). J. Krennder published a report about the *Dobsina* ice cave in 1874. Between 1888 and 1893 E. Fugger published multiple papers about the ice caves of the Salzburg region.

As in 1887 there was already a vast amount of literature on caves available, B. Schwalbe summarized the previous scientific researches and expeditions related to Austrian ice caves. F. Kraus published his work, the *Höhlenkunde* in 1894 that later became the basis for more refined theories about the thermal balance of ice caves. E. Beer and H. Hassinger concluded their findings about the *Geldloch* in *Ötscher* in 1902.

The scientific research of *Dachstein-Rieseneishöhle* started almost immediately after its discovery. Bock and Lahner began the temperature measurements on the 17th of July, 1910. On the 14th of September Saar and A. Hobelsberger descended back to the explored parts of the *Dachstein-Rieseneishöhle* and monitored the temperature and wind movements. In March of 1912, Bock investigated the cave under winter conditions for the first time. The findings were published by Bock and Lahner in their groundbreaking book in 1913. In his work, Bock concentrated on the linkage of the cave climate to the outside weather pattern.

Saar continued on monitoring the cave glaciation between 1920 and 1924. He measured temperature, air humidity and air movements and made estimations of the water condensation levels and the evaporation on the cave walls. These findings were only published together with his later results in 1955 (Saar, 1955).

In 1927 multiple newspaper articles mentioned the serious recession of the cave ice in the *Dachstein-Rieseneishöhle*. The *Bundesministerium für Land- und*

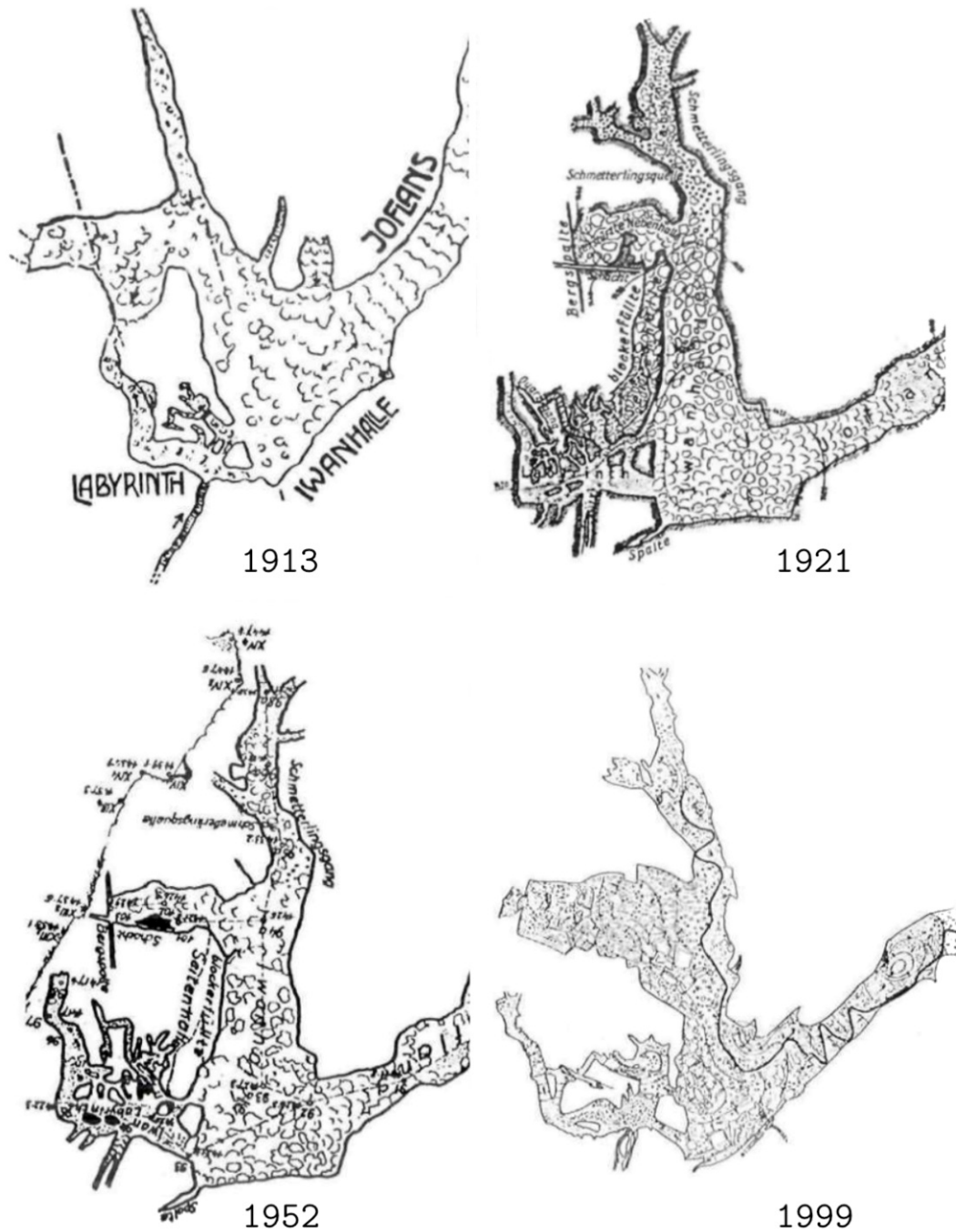


Figure 3.2: Comparison of the different Dachstein-Rieseneishöhle depictions throughout the 20th century. *Notes.* Adapted from “Die speläokartographische Darstellung der Dachstein-Rieseneishöhle im Wandel der Zeit”, Stummer, 1999, p. 146.

Forstwirtschaft ordered an investigation that was led by Prof. Georg Kyrle. The goal was to examine the thermal energy impact of the visiting tourists on the cave climate and whether the incoming thermal energy brought in by the visitors causes the melting.

- They set up 5 weather stations inside the cave and one outside in a weather cabin. The devices were equipped with the standard meteorological sensors of the time, namely thermo-hygrograph, thermometer and two of them also with barometers (one in the outside cabin, the other is in the *Parzivaldom*).
- On five locations they measured the air movements manually but later planted an electrical instrument.
- Thermometers were drilled into the walls on multiple locations with 50. 100 and 150 cm depths.
- For the ground ice measurements instruments were planted in the *Trinstandom* and in the *Parzivaldom* at depths of 50-400 cm.
- Large-format stereo recordings were used to capture the changes of the ice formations during the different times of the year.
- The amount and the quality of the water inside the cave were also monitored on multiple locations.

Although it was a thoroughly planned scientific program, the results were disappointing. Technical problems on a large scale set the progress of the research back. Important measurements were lost due to glitches and another part deemed to be unreliable and imprecise, but despite these difficulties they managed to gather a huge collection of raw data.

Unfortunately the team of Kyrle could not evaluate the collection due to the lack of additional resources and the effort remained as a baseline dataset for the subsequent researches.

After the Second World War, Saar continued his works with the additional findings of Kyrle. He conducted a long-term observation of the *Dachstein-Rieseneishöhle* between 1953-1962. He only had access to limited resources and instruments and focused only on the cave entrance and the *Parzivaldom*.

He carried on the unfinished evaluation of the dataset of Kyrle. Saar was the first who was able to reach back to multiple decades of data and his new results were published in consecutive years from 1953-1956. He concluded that the strongest

correlation seems to be between the lowest temperatures at the given year and the formation of ice inside the cave. Other factors such as the ground temperature, condensation levels and evaporation are less significant.

Chapter 4

Methodology

4.1 Analysis of the literature

The climate of caves has been widely studied in Europe, especially in Central-Europe, but some of the earlier hypotheses about the geographic boundaries of the cave glaciation originate in the former USSR. Although a significant amount of scientific data of the Eurasian caves exist only in Russian, fortunately some of the authors were quoted and translated in english papers (i.e. Turri et al., 2009).

One of the most important sources from Austria regarding this topic is the *DIE HÖHLE - Zeitschrift für Karst und Höhlenkunde* paper. It was first introduced in 1950 and a major part of the studies about the *Dachstein-Rieseneishöhle* were published there over the previous decades. (i.e. Saar, 1954 and Saar, 1957)

The annual reports of the *Forschungswoche* (research seminar) - organized by the *Karst- und höhlenkundliche Abteilung* of the *Naturhistorisches Museum Wien* - are also worth mentioning.

4.2 Data collection

Historical data

The nearest climate stations that are located in the vicinity of the cave are the stations *Schönbergalm* and *Krippenstein*.

In an attempt to have a wider overview of the cave measurements, historical data was gathered not only from online sources but also from the original documents of previous efforts. Multiple stacks of original notes were located from the second Saar-Research (1955-1962). They were photographed and then later digitized. The data

Table 4.1: Weather stations at the *Schönbergalm* and *Krippenstein*.

Station	Location	Measurement	Timestep	Duration
Schönbergalm	N47°32'10" E13°42'59" 1450 m ü.A.	Air temperature	daily/hourly	1957-2020 daily 2005-2018 hourly
		Relative humidity	hourly	2008-2018 hourly
		Precipitation	daily	1957-2020 daily
		Snow depth	daily/hourly	1957-2020 daily 2005-2018 hourly
Krippenstein	N47°31'26" E13°41'39" 2050 m ü.A.	Air temperature	daily/hourly	1957-2020 daily 2008-2018 hourly
		Relative humidity	hourly	2005-2018 hourly
		Precipitation	daily	1957-2020 daily
		Snow depth	daily/hourly	1957-2020 daily 2005-2018 hourly

Air temperature - [°C], relative humidity - [%], precipitation - [mm], snow depth - [cm].

contained mostly daily average air temperature values and daily average relative humidity measurements. Figure 4.1 shows the notes from Saar as they can be found in the archives.

Saar's original measurements from the first research phase (1920-1924) could not be found. More data concerning the 1928-1929 period could be gathered from various sources, such as reports and papers. The daily mean air temperatures were digitized from Saar (1953), while the average values of the monthly mean air temperature of the period between 1920 and 1924 were taken from Saar, 1954. Although the validation of the exact observations is not possible, after importing all the data, the values were manually inspected.

The outliers were removed and not filled. However some of the moving outlier detection and filling methods of *MATLAB* seemed at first promising, I was not able to find the adequate thresholds for the complete automation. Leaving the data free of obvious errors and overextended software correction was an intentional decision.

The locations of the stations used by Saar were compared to the positions of the current monitoring devices as illustrated in Table 4.2. Four of the six stations can be easily matched to a current location. *St. II.* was placed in the *Eiskapelle* part of the *Tristandom*. Currently there are no online stations in that part, so the measurements were compared to those of the *MS 16* at the exit of the *Tristandom*. *St. VI.* was installed in the middle of the *Arthusdom*, whereas the nearest monitoring point is

1962 Blatt 2
 Meteorolog. Stationen Dachsteinrieseneishöhle

	Dat.	22.3.62	24.4.62	29.4.62	2.5.62	15.5.62					
	°C	Zeit	°C	Zeit	°C	Zeit					
I Aussen-Station	Autograph										
	Therm.										
II Eis-Kapelle	Therm.										
III Tristan-Dom	Therm.	-6.2	12.30	-2.0	14.00	-1.4	7.30	-1.4	10.30	+0.4	8.40
IV Parsival-Dom-Station	Autograph										
	Therm.	-5.3	12.0	-3.4	13.50	-2.4	8.55	-1.9	10.25	-1.2	10.25
V Artus-Dom	Therm.	-1.4	11.40	-0.2	13.30	-0.3	7.30	± 0	12.05	+0.4	11.05
VI Pimi-Soel	Therm.	+3.4	11.30	+2.9	12.30	+2.4	7.55	+3.0	12.40	+3.0	11.40
8 Jwanhalle-Extremtherm.	Letzte Korrektur										
	Maximum										
	Minimum										
Wind	Korsca	Ein ← Aus	Ein ← Aus	Ein → Aus	Ein → Aus	Ein ← Aus	Ein ← Aus				
	Ob. Eing.	Ein ← Aus	Ein ← Aus	Ein → Aus	Ein → Aus	Ein ← Aus	Ein ← Aus				
	Kageschl.	Para. → Art.	Para. → Art.	Para. → Art.	Para. → Art.	Para. → Art.	Para. → Art.				

Allg. Wettercharakter Obertags, besonders in der Höhle:
 22.3.62 *Wühl-Lunneblö*
 9.4.62 *bedeckt, Schauer*
 14.4.62 *bedeckt, Föhn*
 2.5.62 *bedeckt, Schneefall, Stirmwind*
 15.5.62 *bedeckt, leichter Schneefall*

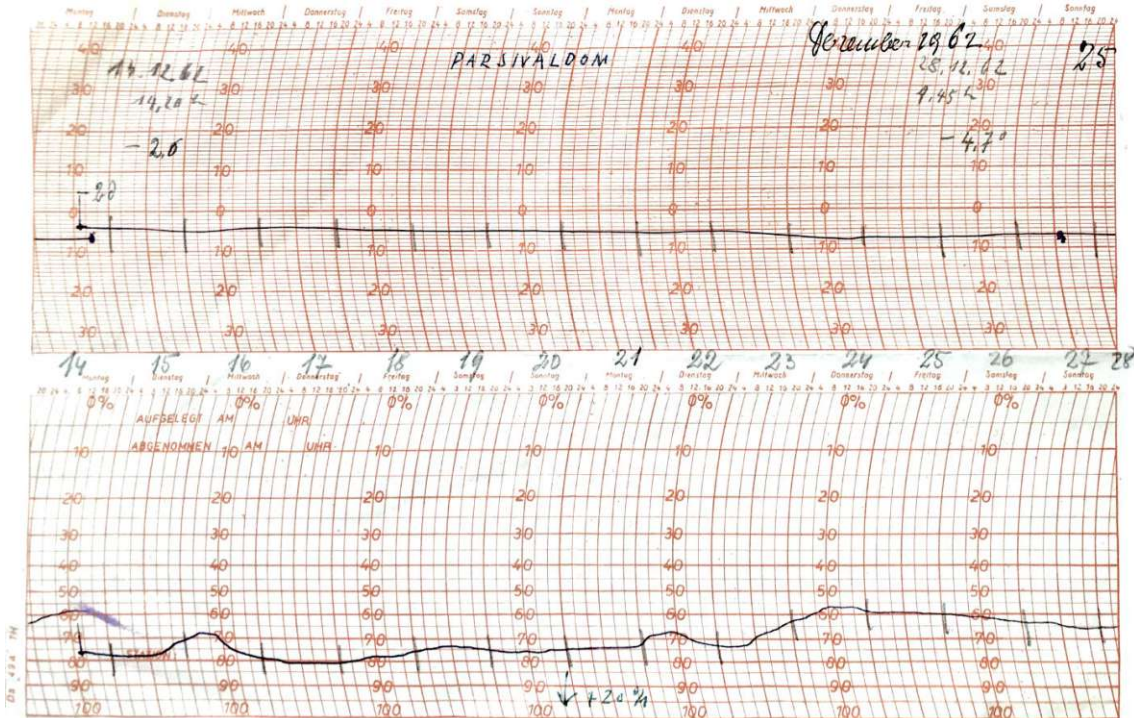
Speleologisches Institut Dachstein-Rieseneishöhle
 Temperaturblatt 1960
 Station: Parsivaldom Monat: Februar

Tag	Temperatur °C				Extremwerte		Bogenmaß	Anmerkung	Absolutes Instrument		
	2*	7*	10*	21*	Maximum °C	Minimum °C			Tag	Stunde	°C
1	-2.4										
2											
3											
4											
5	-2.3	-2.2	-2.2	-2.3							
6	-2.3	-2.5	-2.4	-2.5							
7	-3.3	-3.0	-3.0	-3.5							
8	-4.5	-4.4	-4.3	-4.5							
9	-4.5	-4.2	-4.1	-3.0							
10	-3.0	-3.0	-3.0	-3.4							
11	-3.4	-3.2	-3.0	-2.8							
12	-2.8	-2.7	-2.6	-2.5							
13	-2.5	-2.5	-3.0	-2.5							
14	-2.5	-2.2	-2.9	-3.0							
15	-3.5			-3.0							
16	-2.8			-2.8							
17	-2.8			-2.8							
18	-2.8	-2.6	-2.7	-2.6							
19	-2.2			-2.2							
20	-2.2	-2.2	-2.2	-2.4							
21	-2.4	-2.4	-2.4	-2.4							
22	-2.4	-2.4	-2.3	-2.3							
23	-2.3			-2.3							
24	-2.3			-2.3							
25	-2.3	-2.3	-2.7	-2.0							
26	-2.0	-1.8	-1.8	-2.0							
27	-1.7	-1.7									
28			-1.7								
29				-1.7							
30											
31											

Perladen	Summe	Mittel °C
1.-5.	-11.9	-2.4
6.-10.	-18.7	-3.7
11.-15.	-14.2	-2.8
16.-20.	-22.6	-4.5
21.-25.	-11.5	-2.3
26.-	-7.1	-1.8
Monatsmittel	-2.6	
Frosttage: 29		%
Eistage: 29		%

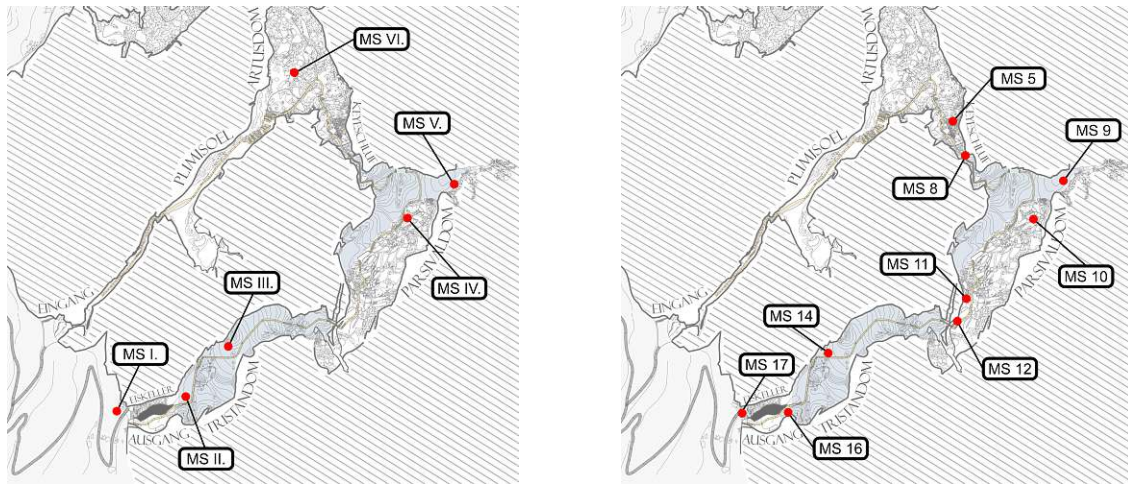
(a) Aggregat from multiple stations

(b) Daily measurements from one station



(c) Results from the original automated weather station. 1962. (Thermometer-Hygrometer with Autograph)

Figure 4.1: Examples of the original notes from the Saar team that worked in the cave between 1955 and 1962. They were scanned in 2019.



(a) Location of the weather stations used by Saar

(b) Location of the current weather stations.

Figure 4.2: The current online weather stations are depicted on the right side. Additionally ice, water and rock temperatures are also measured in different locations in the *Parsivaldom* and in the *Kreuzgang*.

at the south-eastern end of the hall, next to the *Keyeschluf*. The maps side-by-side can be seen in Fig. 4.2.

Table 4.2: Comparison of the current and past monitoring locations.

Location	MS ID	D	Saar ID	D
Arthusdom	MS 5	400 m	St. VI.	435 m
	MS 8	380 m		
Parsivaldom	MS 9	340 m	St. V.	340 m
	MS 10	300 m	St. IV.	300 m
	MS 11	180 m		
Kreuzgang	MS 12	160 m		
Tristandom	MS 14	90 m	St. III.	100 m
	MS 16	20 m	St. II.	60 m
Eiskeller	MS 17	0 m	St. I.	0 m

MS ID - current designation of the active monitoring points that were used for the historical comparison. D - distance from the exit at the *Tristandom*. Saar ID - station names and locations that were used by Saar.

Between July of 1928 and September of 1929 almost 450 days were monitored. According to Saar (1955) the daily averages were calculated not only with the *Mannheimer Stunden* (7h, 14h, 21h) but an extra measurement at 2h was also taken into account. As Equation 4.1 indicates, it puts an emphasis on the cooling effect of the night. Kyrle started using this method after the first exploration.

$$\frac{T_{7:00} + T_{14:00} + T_{21:00} + T_{02:00}}{4} \quad (4.1)$$

The notes that were taken between 1955 and 1962 show that the so called *Kämtzisches Mittel* was also used for the aggregation of the daily average. This method uses the *Mannheimer Stunden*, but calculates the 21h value twice as seen in Equation 4.2.

$$\frac{T_{7:00} + T_{14:00} + 2 \times T_{21:00}}{4} \quad (4.2)$$

Current data

The dataset that I worked with, was the result of an ongoing effort from the management of the *Dachstein-Rieseneishöhle*. Approximately 15 monitoring stations were mounted in the main halls of the cave. These are online stations, connected to a server and record a value once every hour. Four stations record besides air temperature and relative humidity, the air flow velocity and direction as well. After August of 2018, some of the non-functioning stations were moved or disassembled. Table 4.3 shows the current online measuring setup.

The air temperature measuring sensors are the *EE071* by *E+E*. They have an accuracy of $\pm 0.4^\circ\text{C}$ between -10°C and 0°C . The relative humidity accuracy is $\pm 2\%$ until 90% and $\pm 3\%$ above 90%. The instruments are also fitted with a radiation shield.

4.3 Data quality

The observations were imported into and analyzed in *MATLAB* and organized into a `struct` in a `timetable` format. The hourly and sub-hourly values were resampled with the `retime` function, using `mean` as the aggregation method. The hourly data could be then easily synchronized between the different stations and did not require additional interpolations.

The data of the *Schönbergalm* and the *Krippenstein* were kindly provided by the *Dachstein Tourismus AG* (DAG) and the *Lawinenwarndienst Oberösterreich*. Measurements since the fifties were included in the packages and they are of high quality, cleaned of obvious equipment errors.

Table 4.3: Locations of the online weather stations.

Location	MS ID	D	Measurement	Validation
Arthusdom	MS 5	400 m	Air temperature	x
			Relative humidity	
Parsivaldom	MS 8	380 m	Air velocity	
			Airflow direction	
	MS 9	340 m	Air temperature	x
			Relative humidity	
MS 10	300 m	Air velocity		
		Airflow direction		
Kreuzgang	MS 11	180 m	Air temperature	x
			Relative humidity	
			Air velocity	
Tristandom	MS 12	160 m	Airflow direction	x
Eiskeller	MS 14	90m	Air temperature	x
			Relative humidity	
			Air velocity	
Tristandom	MS 16	20 m	Airflow direction	x
Eiskeller	MS 17	0 m	Air temperature	
			Relative humidity	

MS ID - current designation of the active monitoring points that were used in the evaluation. D - distance from the exit at the *Tristandom*. Saar ID - station names and locations that were used by Saar. Validation - shows which measurements were validated with an additional offline datalogger.

Chapter 5

Results of the monitoring

As described in the previous chapter, all the data was prepared in *MATLAB*. For the evaluation, the outliers were only removed and not replaced with any aggregation methods.

The daily frequency was the most used sampling rate. It has enough resolution for the detection of significant anomalies. For the inspection of longer trends, the mean monthly air temperature was used (resampled from the daily values where it was available).

In the monitoring period since 2017 high quality hourly observations are also available.

5.1 Cave climate regimes

Two distinct patterns of the cave microclimate could be observed in the *Dachstein-Rieseneishöhle*. This classification allows a more focused approach investigating the cave glaciation. Figure 5.1 illustrates the difference between the summer and winter regimes. The wind direction in the cave helps identifying the turning points:

- Summer regime: May, June, July, August, September and October
- Winter regime: November, December, January, February, March and April

The regional weather pattern seems to be less definite around May and November, but for the purpose of this comparison, the above mentioned grouping was used for the statistics. The same classification was also used in studies about the *Eisriesenwelt* by Obleitner and Spötl (2011).

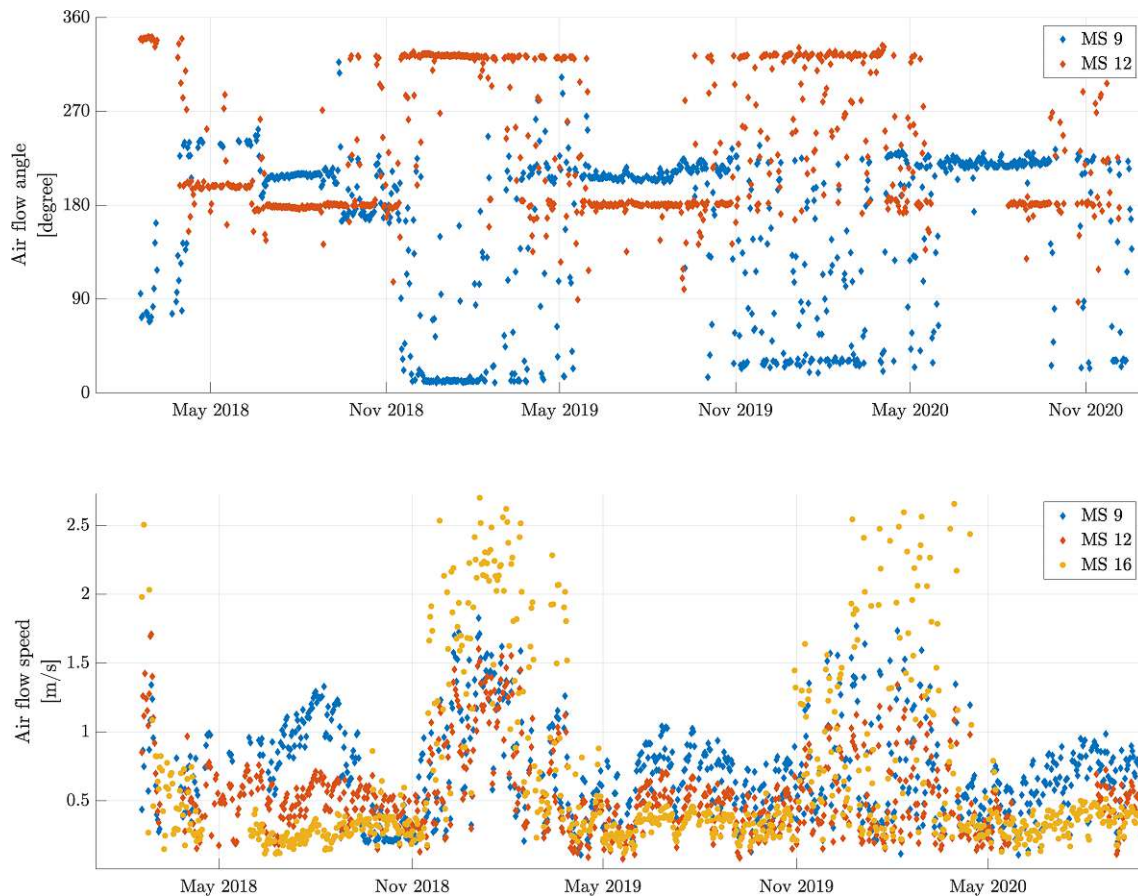


Figure 5.1: Air flow direction and velocity in the cave. The *MS 9* is located at the *Versturz*, while the *MS 12* is at the *Kreuzgang*.

Figure 5.2 depicts the seasonal average air temperatures at the weather stations. The colors are a rough interpolation that helps illustrate the geometrical context of the measurements.

In the last couple of decades, the transitional periods of the cave regimes show a greater increase in the mean air temperature according to the data recorded by the *Lawinenwarndienst*. Figure 5.3 compares the mean monthly temperature values in the winter regime where $T_{MMAT} \geq 0^\circ\text{C}$. It suggests that high temperatures in April and November became more frequent since 1957. This presents a clear danger to the cave glaciation.

5.2 Trends in the region

The rate and the direction of the temperature changes in the Alps have been widely investigated. The research indicates, that ice accumulation on longer timescale is decreasing. As highlighted by the analysis of Gobiet et al. (2014), the changes in the regional climate will be significant until the end of this century. He argues, that an estimated $0,25^\circ\text{C}$ rise in the annual temperature in the following decades is to

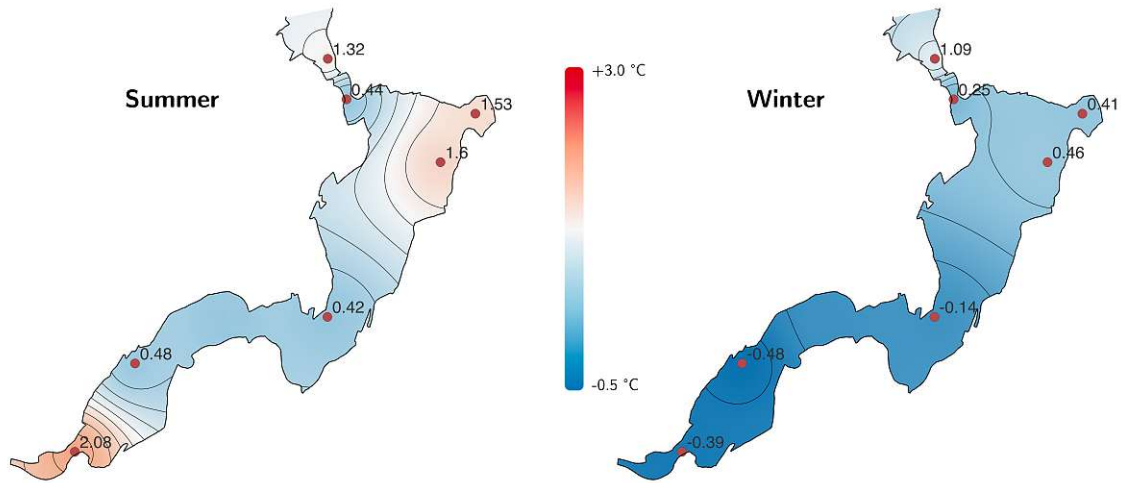


Figure 5.2: Mean air temperature in the different regimes at the current measuring stations. The heatmap was interpolated from the aggregated measurement values of the stations in QGIS 3.20.

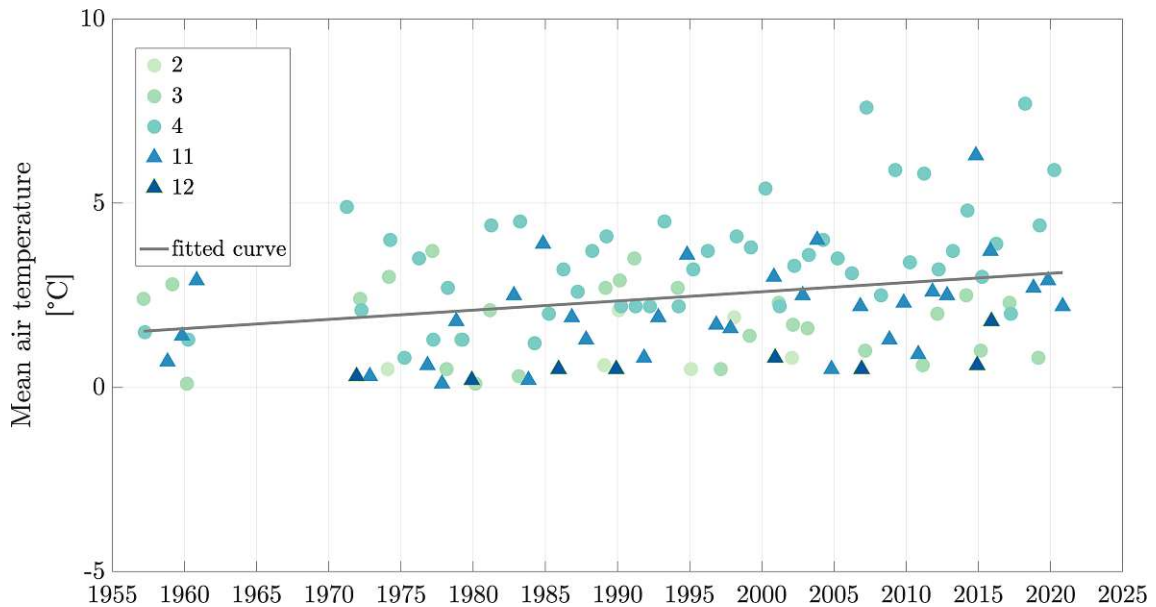


Figure 5.3: Mean monthly air temperature values in the transitional months at the *Schönbergalm*.

be expected. The rise will be getting quicker ($0,36^{\circ}\text{C}$) after 2050. According to his most likely scenario, temperature extremes are to be expected every other year.

The mean monthly air temperature trends of the *Schönbergalm* and the *Krippenstein* stations between 1957 and 2020 are in line with the findings of Gobiet. Figure 5.4 indicates a steady increase in the mean temperatures of the summer and winter periods. Assuming that the linkage between the changes in the mean temperatures and the timeline is linear, a simple regression model was fitted on both summer and winter regimes at the two locations. The regression slopes revealed that the increase in the summer regimes were about $0,026^{\circ}\text{C}$ a year in both cases. The winter regimes have a smaller inclination with $0,019^{\circ}\text{C}$ a year at *Krippenstein* and $0,014^{\circ}\text{C}$ a year at *Schönbergalm*. This outcome supports the results from Gobiet. It is important to state, that this basic linear fitting provides valuable information only about the past decades and is not a tool to predict any future increase in the mean air temperature.

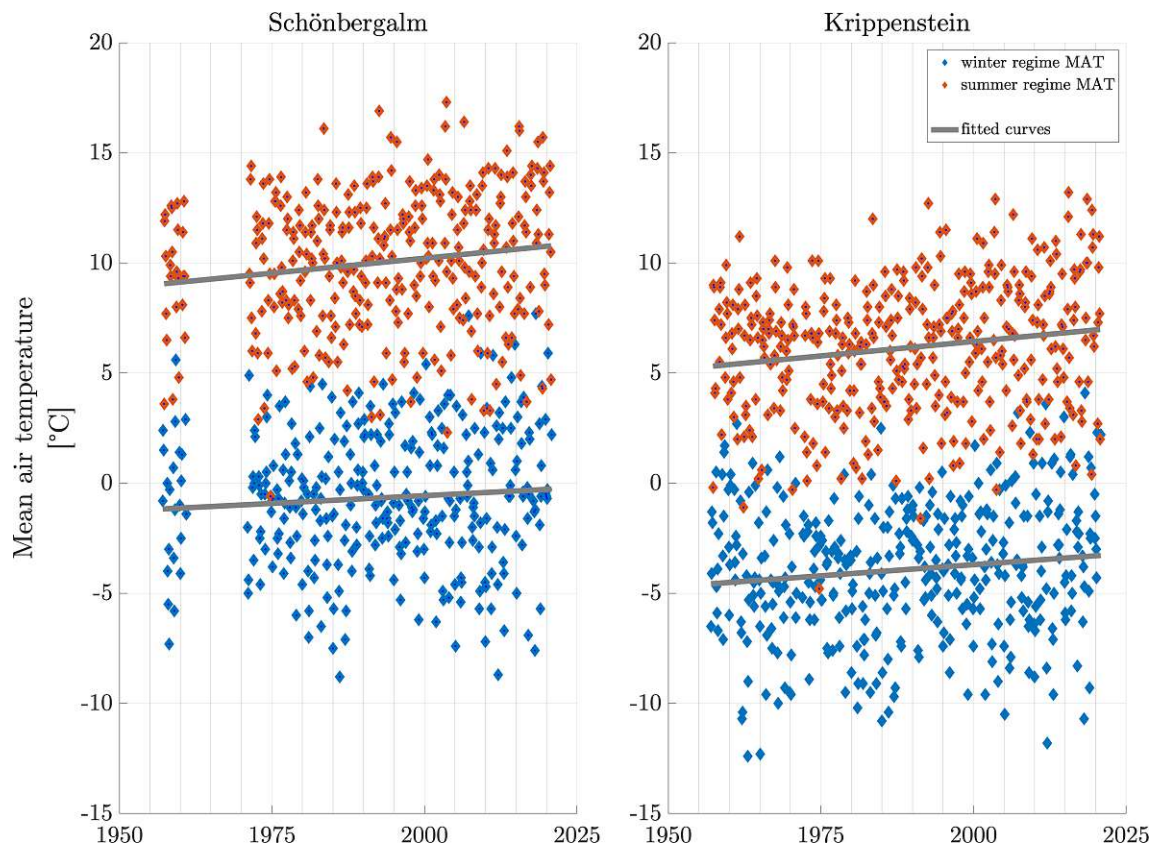


Figure 5.4: Mean air temperature of the winter and summer regimes of the *Schönbergalm* and *Krippenstein* stations

Strong evidence of the temperature increase on a longer timescale was also found in the cumulative distribution of the measurements. As highlighted in Fig. 5.5, significant differences can be observed between the mean monthly air temperatures from the seventies and the past decade. The period between 1971–1980 was selected,

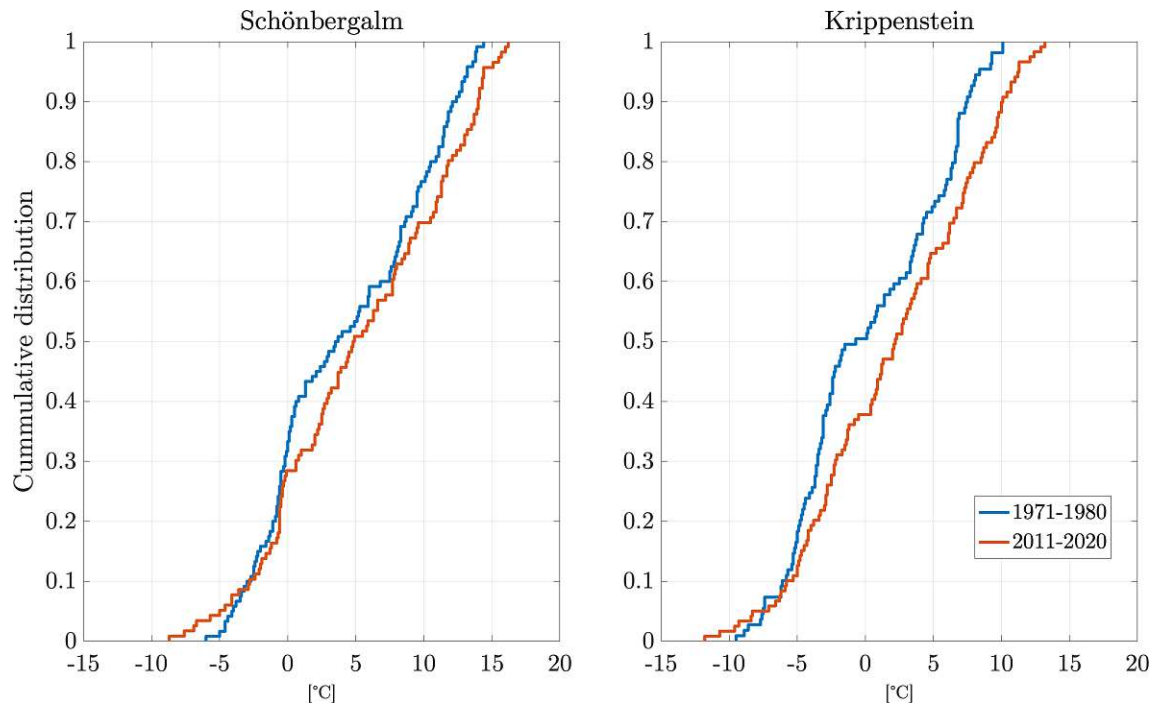


Figure 5.5: Cumulative distribution of the temperature measurements at the *Schönbergalm* and *Krippenstein* stations.

because this is the only almost complete dataset before 1990, that is comparable to the years of 2011-2020.

Projections of Gobiet also indicate that temperature extremes are becoming more frequent, especially towards the end of this century. An upward trend of the standard deviation - calculated by grouping the values by year and by regimes - can be observed in Fig. 5.6. Higher *SD* values have been more frequent in the last 20 years, especially in the winter periods. This rate is even bigger than the apparent mean temperature increase.

As some previous studies predicted, climate change rate might have an altitude gradient regarding some aspects. At higher altitudes a more “anomalous warming” should be expected, but at lower altitudes the retreat of the snow coverage could amplify the temperature rise, notably under 1500-2000 m. The data collected from the *Dachstein-Rieseneishöle* suggest that the temperature differences of the *Schönbergalm* (1458 m) and the *Krippenstein* station (2050 m) were not diverging that much in the past decades. It is apparent from Fig. 5.7 that there was a general dip after 1983, but since then, the difference is usually around 3°C during the winter months and 3,5°C in the summer, except the year of 2017.

The 6°C mean temperature difference was due to the extremes in the *Schönbergalm*. The amplitude of the winter temperature graphs is bigger in general, but the 500

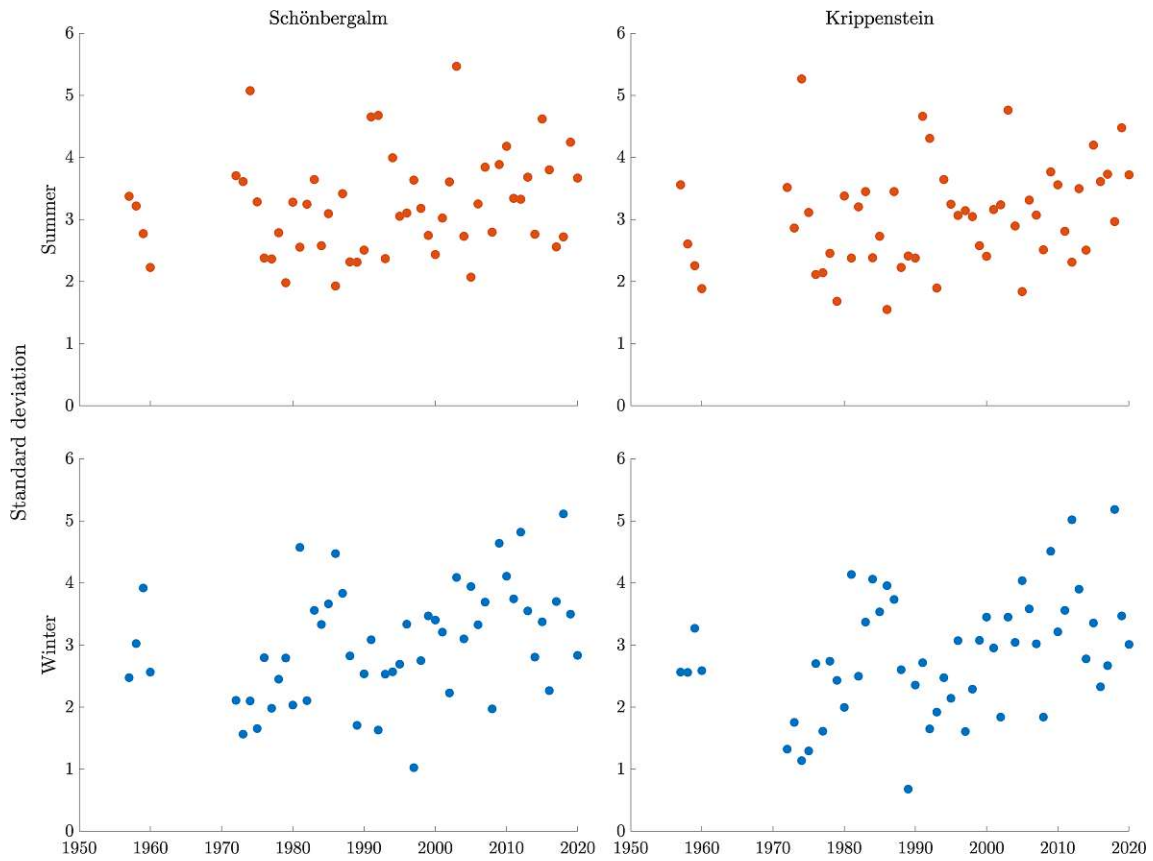


Figure 5.6: Standard deviation of the aggregated measurements of the *Schönbergalm* and *Krippenstein* stations.

m altitude difference between the stations might indicate an even bigger variance. (See Fig. 5.7.)

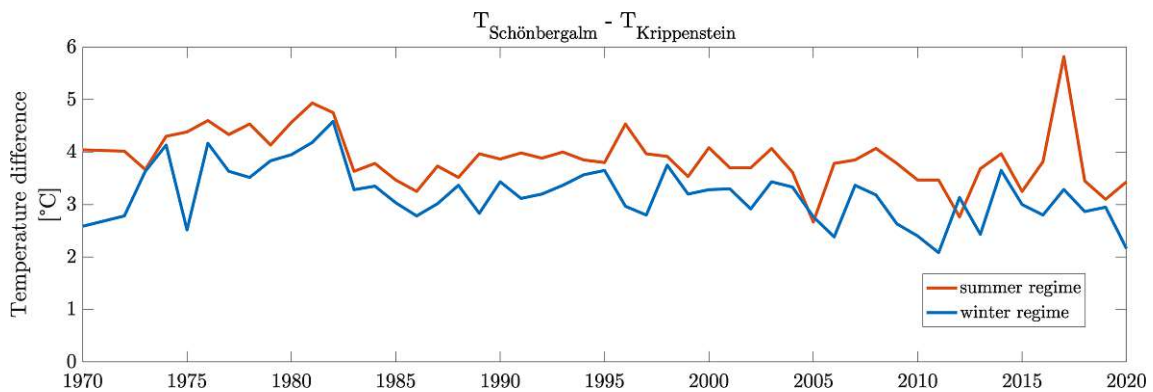


Figure 5.7: Mean temperature differences between *Schönbergalm* and *Krippenstein*. One datapoint shows one aggregated winter or summer period.

A rising rate of the annual sum precipitation in the summer months can be observed in Fig. 5.9, that correlates with the regional climate change predictions. The results show that the extreme values of precipitation in the warmer period can be a great amount of heat source.

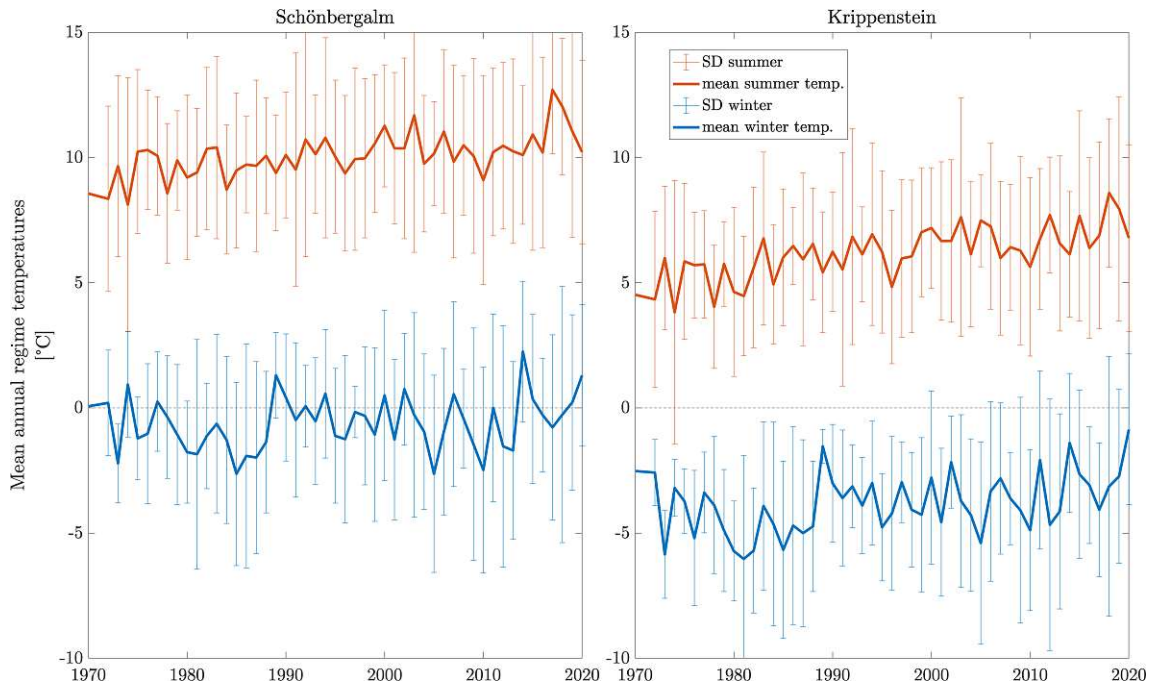


Figure 5.8: Mean annual air temperatures aggregated by the summer and winter regimes. The error bar shows the standard deviation.

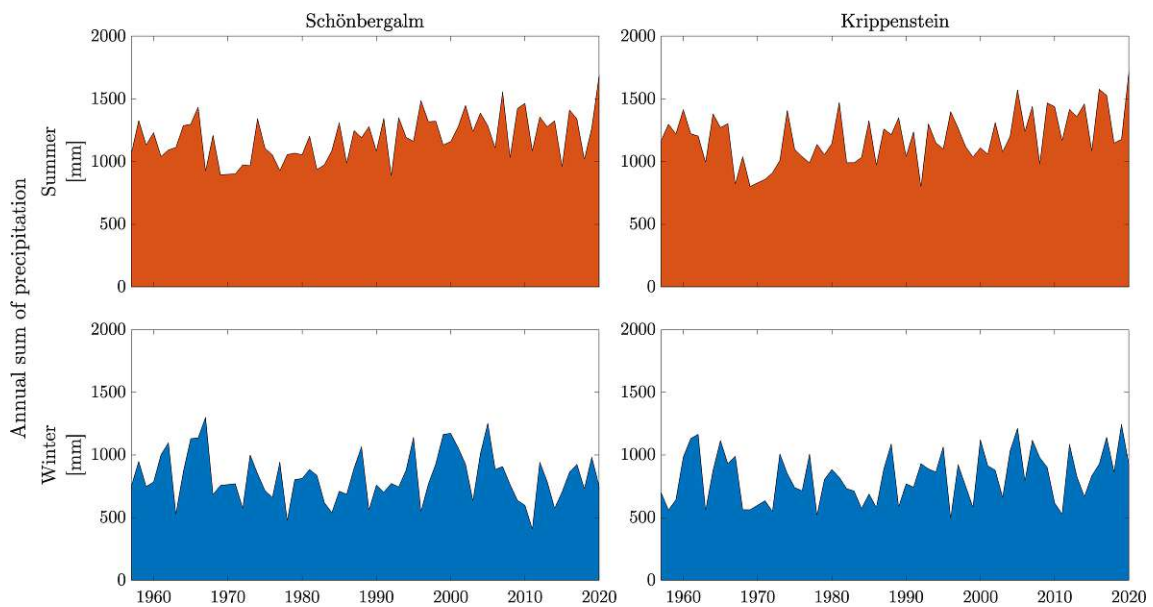


Figure 5.9: Annual precipitation in the different regimes at the *Schönbergalm* and *Krippenstein* stations.

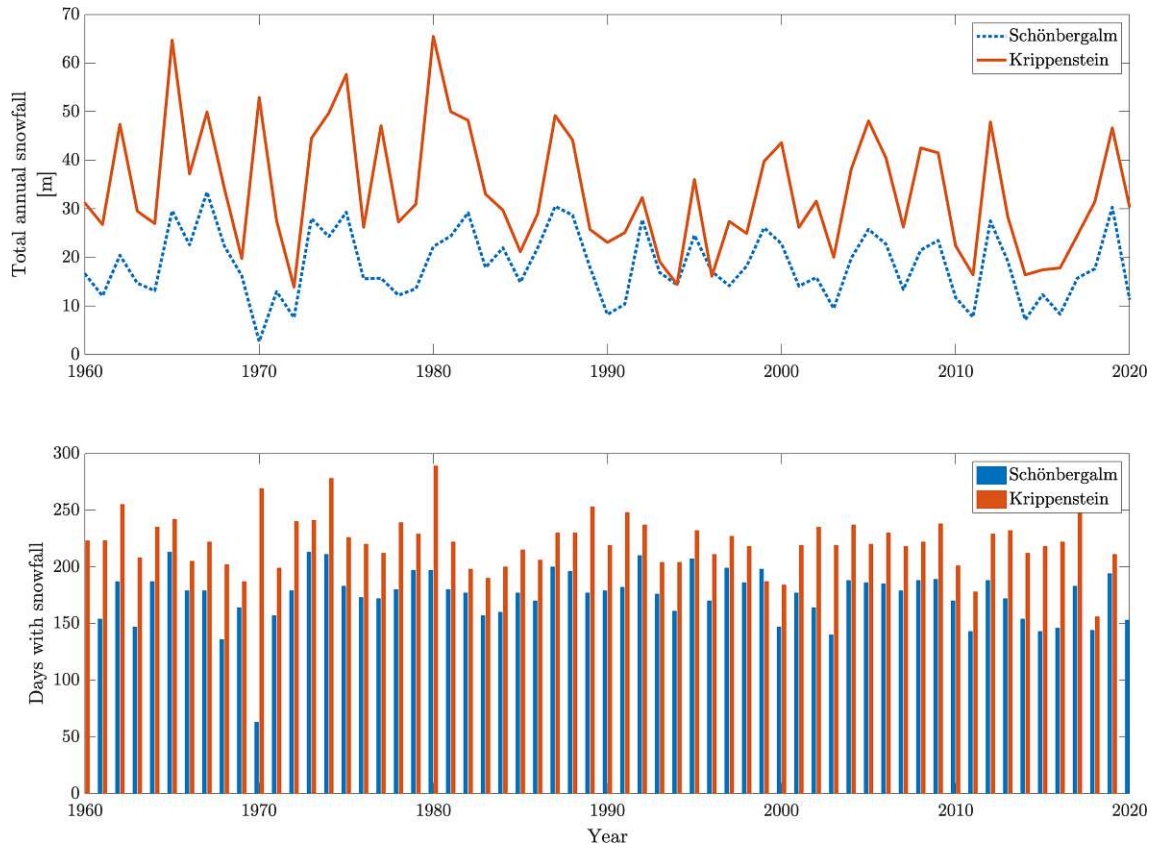


Figure 5.10: Annual snowfall measurements at the *Schönbergalm* and *Krippenstein* stations.

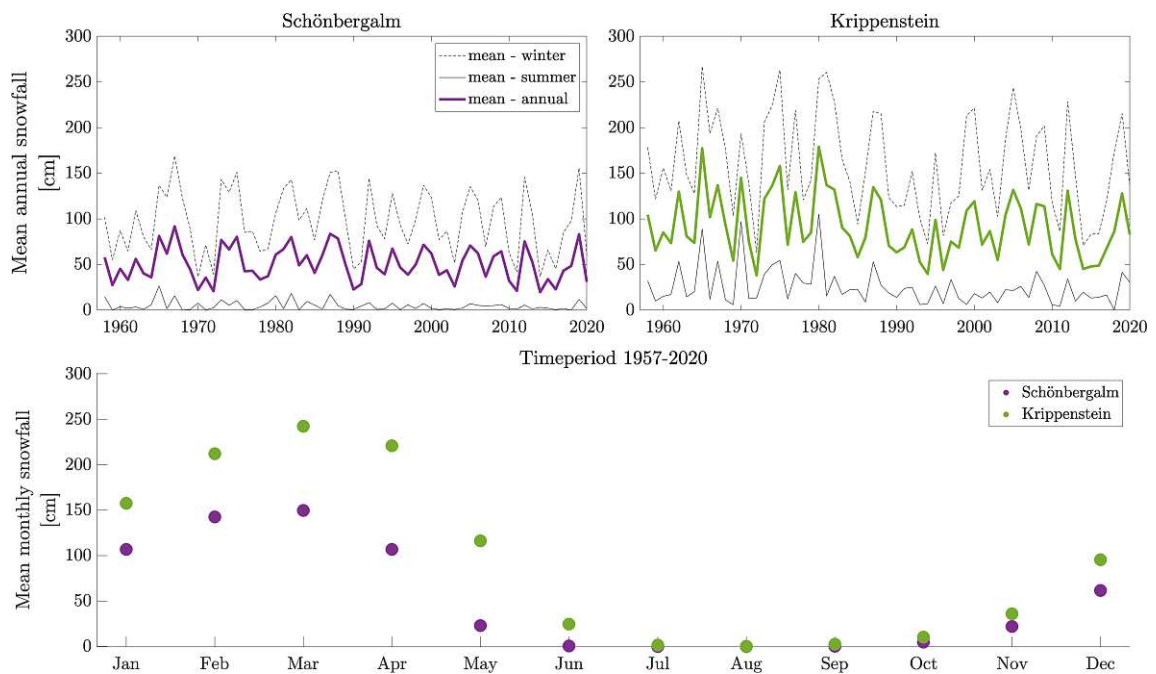


Figure 5.11: Snowfall measurements at the *Schönbergalm* and *Krippenstein* stations. The upper part illustrates the average values with the minima and maxima at the given year, while the bottom graph depicts the monthly distribution of the averages.

5.3 Annual trends

The weather station St. IV. by Saar and the current MS 10 have almost the same location in the *Parsivaldom* and they both have the most daily data available. The old observations were digitized from the original notes. These documents suggest that the daily mean temperature was calculated using the *Kämtzsches Mittel*. Since the current logging began in 2018, the daily value has been calculated from the mean of the 24 hourly recordings. Figure 5.12 demonstrates a significant temperature increase in the last seven decades.

The *Parsivaldom* is the deepest of the main halls that contains perennial ice in the *Dachstein-Rieseneishöhle*. The years of 2019 and 2020 show two winter periods that were almost exclusively above the glaciation temperature range. Unfortunately, the measurements in 2019 were not complete due to sensor error, but the data of the first 60 days suggest no significant cooling effects took place in January and February.

The number of frost days in the *Parsivaldom* since 1928 are in line with the mean monthly air temperature values. As detailed in Table 5.1, on average less than 40 frost days have been recorded in the last few years. This value in the fifties was more than 350 days according to the observations of Saar.

Looking at Fig. 5.13, the monthly temperature differences at *Schönbergalm* might not seem significant. Comparing it to the changes in the *Parsivaldom* indicates that the local climate in the last three years has not been significantly warmer than the reference timespan in the fifties. Although, it can be observed that the summer regime was hotter in the period of 2018-2020 than between 1957 and 1959, the mean temperature at the *Schönbergalm* alone does not explain such a contrast in the deeper parts of the cave.

It is probably a process, in which the rising annual air temperature of the region translates to a warmer water influx besides the less cool winter air and the ever warming summer heat influx. Throughout the years the ice cover slowly retreats, which changes the latent heat balance and thermal energy budget of the cave microclimate.

Figure 5.14 demonstrates the aggregated annual temperatures at the observing stations between 2017 and 2020 in relation to distance into the cave. A significant rise in the values at the *Versturz* (MS 9) is a clear indication that a large amount of thermal influx coming through that part of the cave is responsible for warming up the deepest part of the *Parsivaldom* (MS 10). Airflows enter at a low altitude next to the *Versturz* and have a visible influence on the thermal balance of the *Parsivaldom*.

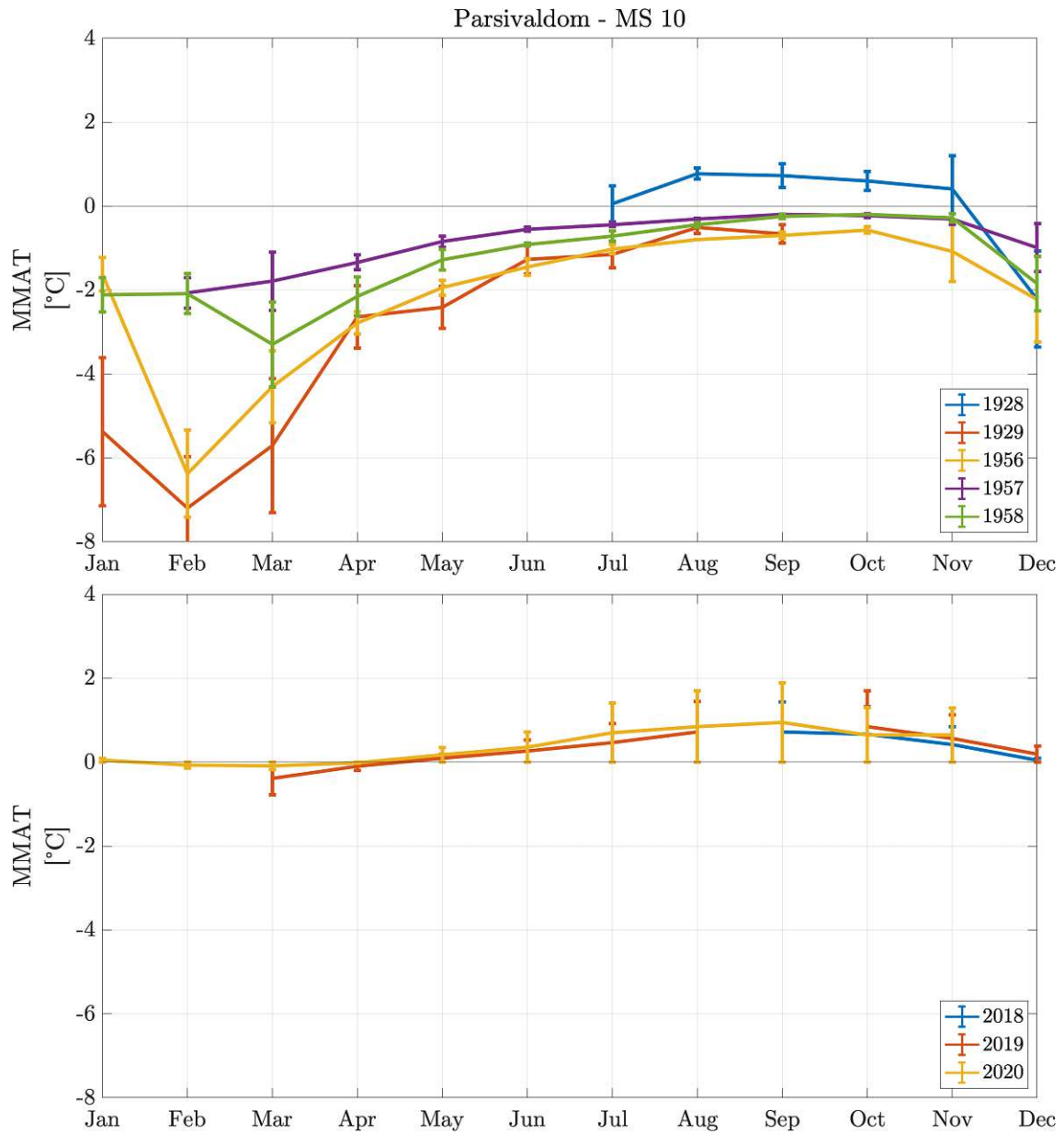


Figure 5.12: Mean monthly air temperature in the *Parsivaldom*. The error bar shows the standard deviation.

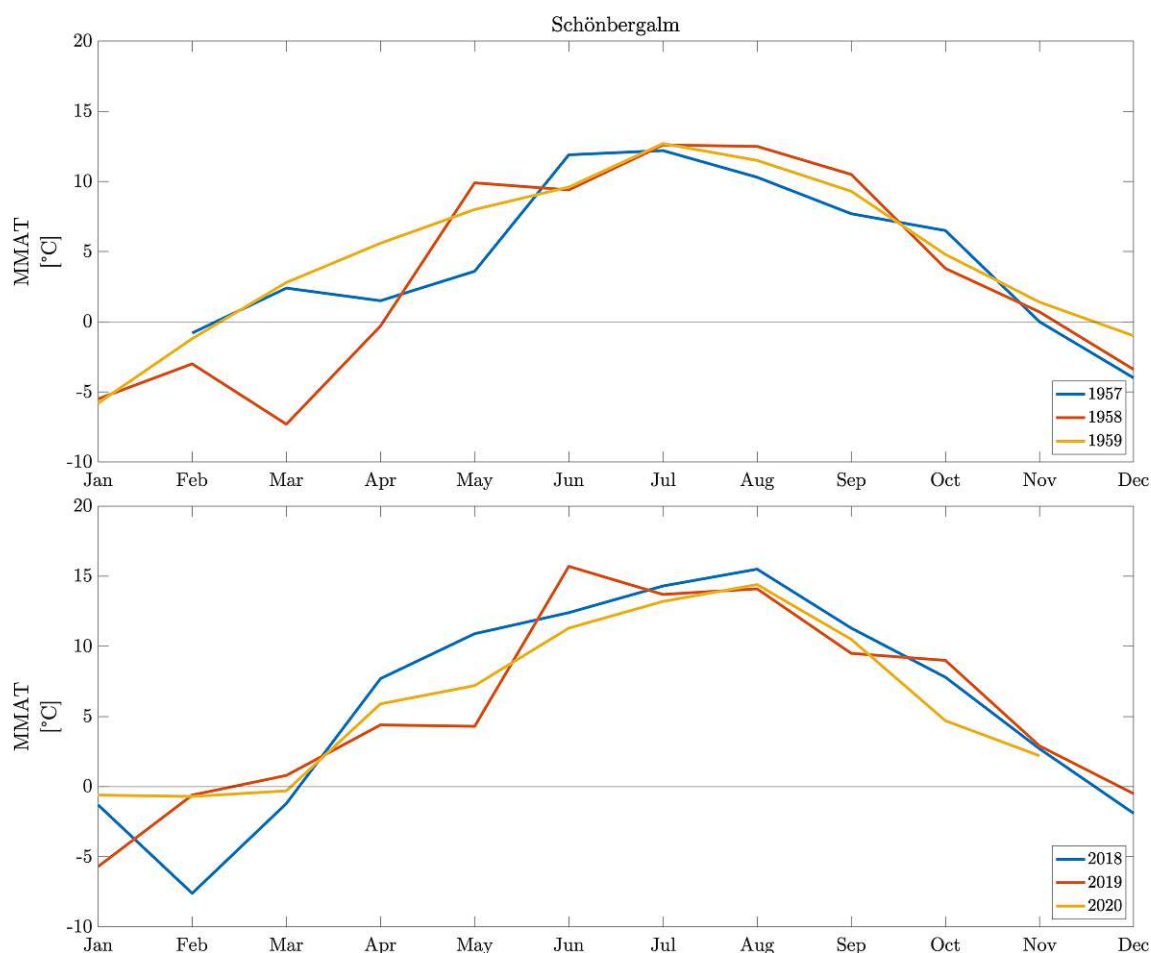


Figure 5.13: Mean annual air temperatures grouped by the observation periods of 1957-59 and 2018-20.

Table 5.1: Frost days in the *Parsivaldom* (at MS 10)

	Jan	Feb	Mar	Apr	May	Jun	Jul	Aug	Sep	Oct	Nov	Dec	Σ
1928	-	-	-	-	-	-	-	0	0	0	7	31	38
1929	31	28	31	30	31	30	31	31	26	-	-	-	269
1956	31	29	31	30	31	30	31	31	30	31	30	31	366
1957	-	28	31	30	31	30	31	31	30	31	30	28	331
1958	31	28	31	30	31	30	31	31	30	31	30	31	365
2018	26	25	-	-	-	0	0	0	0	0	0	0	51
2019	9	2	4	3	2	0	0	0	-	1	2	5	28
2020	2	10	12	10	0	0	0	0	0	0	-	-	34

FD - Frost day. It is measured by the mean daily air temperature. It is considered to be a frost day, where the average is below 0°C.

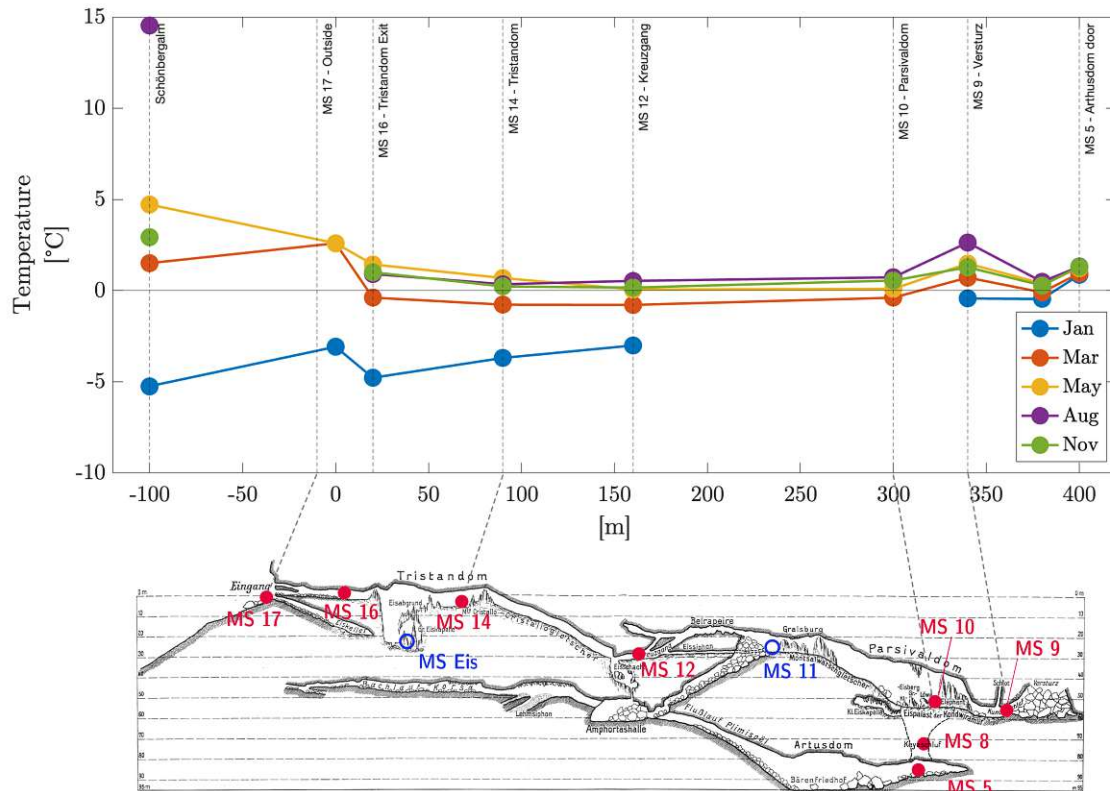


Figure 5.14: Mean monthly air temperature at the observing stations between 2017 and 2020 in relation to distance into the cave.

Both summer and winter periods show the effect of the influxes at the *Versturz*. From Fig. 5.15 it can be noted that the horizontal temperature gradient near the entrance is less elevated in winter than in summer. As previously discussed, it belongs to the heterothermic zone of the cave, where the temperatures show a high seasonal variation.

It is important to mention that the current measurements are made with at least two sensors. After validation, correction was needed throughout 2018 and 2019. Probably similar errors with the instruments could have happened in the previous decades, therefore these values without any validation should be used carefully. The trends and the winter cooling rates on the other hand can be compared between the different decades. The current winter regimes demonstrate a much lower amplitude regarding the temperature rates. It is a clear indication, that the cave might need more inwards flowing air mass in order to have a stable glaciation period.

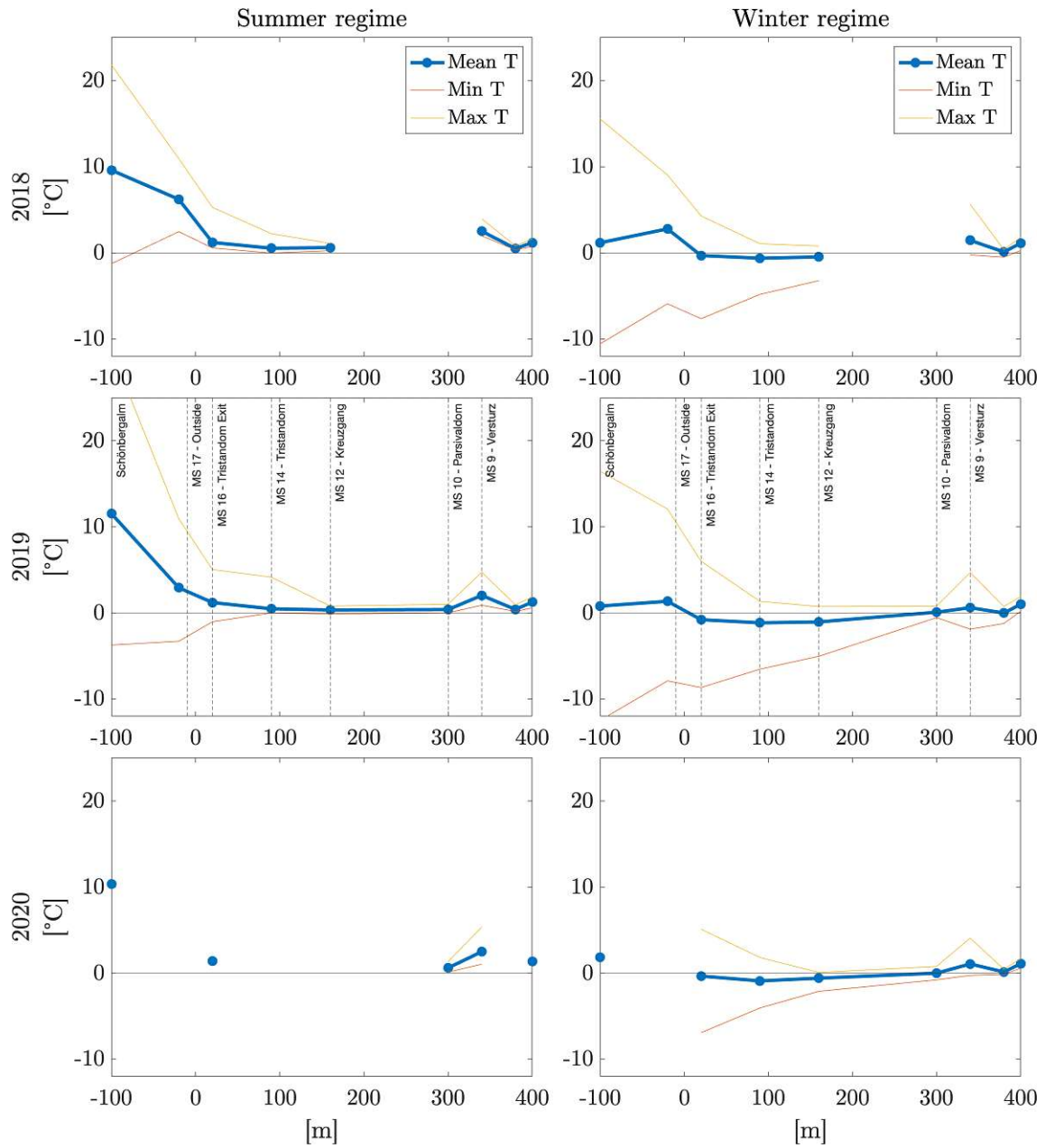


Figure 5.15: Mean temperatures aggregated by the summer and winter regimes in the period of 2018-2020 and compared to the station distance from the cave entrance.

Chapter 6

Ice cave models

Modeling the complex nature of cave microclimates is a challenging task, mostly due to the karst characteristics. The sheer amount of unknown variables regarding the thermal energy influxes make it difficult to have a controlled environment where a model could be verified. The ice mass can signal the overall energy and mass balance of the cave that can serve as a metric of validation.

6.1 First approaches

The phenomenon of ice in cave formations during the warmer seasons have been already reported since the 15th century. The thorough scientific study started only later, during the second half of the 19th century (Meyer, 2018).

The first ice cave theory was mentioned in the late 16th century by Poissenot (as cited in Fugger, 1893). He argued that the subterranean ice develops during the winter season and the warm summer air can not penetrate deep behind the cave entrance. This theory remained the base of the accepted explanations. Until the late 19th century it had been believed that the ice might form only in the summer season due to evaporation caused by higher summer air flow rates. This assumption has been proven to be false by more exhaustive observations. In the early 18th century Billerez considered whether the ice formations are caused by salt solution.

Later that century the chemical analysis showed that there is no extensive salt concentration in the water of ice caves. As cited in Fugger, 1893, Parrot points out in 1815 that the caves had a steady temperature regime where an evaporative cooling effect might explain the presence of ice in the summer months. The warm and dry air flowing into reaves could lead to a cold enough microclimate for a stable glaciation period. After multiple observations in french ice caves the theory was disproven (Balch, 1900).

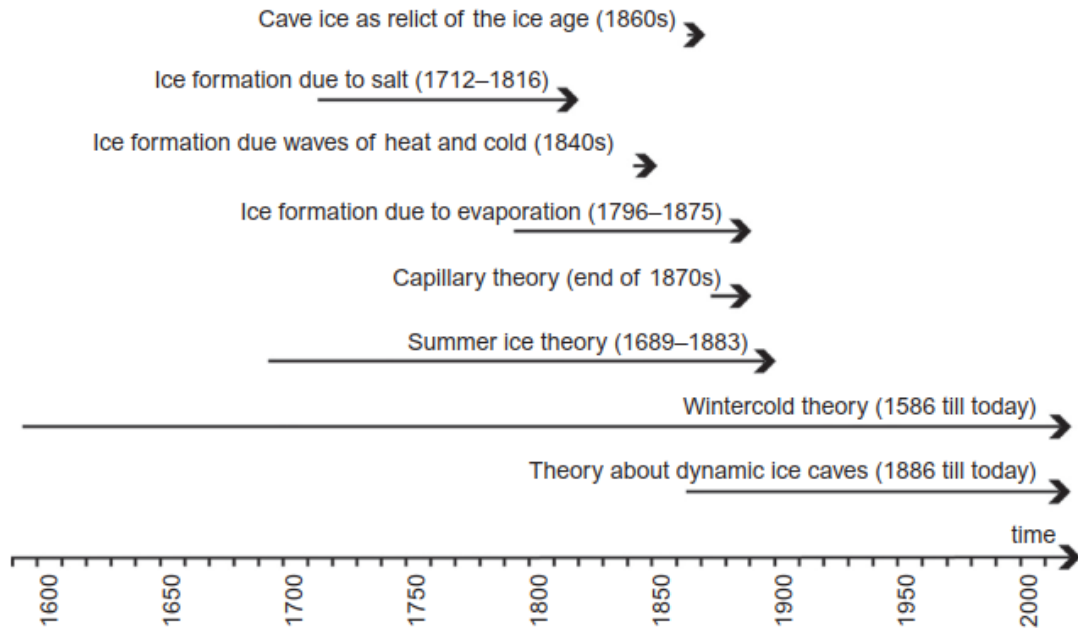


Figure 6.1: Chronology of the different theories regarding the ice cave phenomenon. *Notes.* Reprinted from “Reports on ice caves in literature from the twelfth to the middle of the twentieth century”, Meyer et al., 2017, p. 144.

Early on scientists had to face the problem of classification regarding ice caves. Thuri, as cited in Bock et al., 1913, started the scientific work with establishing the terminology of static and dynamic ice caves, which is still used today.

6.2 Mass and energy balance

The ice accumulation in a given period can be measured by the thickness and the density changes of the ice body. The mass balance is a combination of accumulation and ablation. Accumulation can occur due to freezing or direct deposit, whereas ablation comes from the ice evaporation and melt. The specific mass balance equation in a reference period $t_1 - t_2$:

$$b = \int_{t_2}^{t_1} \frac{\partial c + \partial a}{\partial t} = \int_{t_2}^{t_1} \rho \times \frac{dh}{dt} \quad (\text{kg} \cdot \text{m}^{-2}) \quad (6.1)$$

where b is the mass balance per unit area, c is the specific accumulation, while a is the specific ablation. It can be translated to the changes in the height of the ice body, h and the density of the ice, ρ . The density can be assumed constant in a cave environment with $920 \text{ kg} \cdot \text{m}^{-3}$ (Schöner et al., 2011).

The mass balance can be derived from the following one-dimensional numerical energy balance model and equation (Jordan, 1991):

$$\begin{aligned}\frac{dE}{dt} &= NR + SHF + LHF + S + PHF \\ &= \int_{z=0}^H \left(\frac{d}{dt} (c_p \rho(z) T(z)) \right) dz + L_V R_{F,M} \quad (\text{W.m}^{-2})\end{aligned}\quad (6.2)$$

where E illustrates the internal energy change in the ice mass, NR is the net radiation on the surface, SHF is the sensible heat flux, LHF is the latent heat flux, S represents the heat flux in the ice body and PHF is the heat flux due to the seepage water (precipitation). The right hand side of the equation describes the different processes associated with heat and vapor diffusion, water transport and latent heat exchanges (Obleitner & Spötl, 2011).

Ice surfaces are usually not directly impacted with short wave radiation, therefore NR can be described by the long wave components. According to Obleitner and Spötl (2011) measurements at the *Eisriesenwelt* indicates that the net radiation is the most significant energy input at various periods. In March it is measured to be around 0 W.m^{-2} , but in August it rises to around 2 W.m^{-2} .

In his analysis of the *Monlesi* cave in Switzerland, Luetscher et al. (2008) suggests a similar approach. His thermodynamic reference point is taken at the melting point of pure ice. The boundary conditions are the external climate and the cave rock temperature. The heat exchanges occur as (I) conduction through the cave walls, (II) sensible and latent heat advection by air and water circulation and (III) solar radiation. This model is characterized by the following equation:

$$\Delta E_{air} + E_{rock} + \Delta E_{water} + LE_{snow} + R = \Delta SE_{ice} + \Delta LE_{ice} \quad (6.3)$$

where ΔE_{air} is the sensible and latent heat advected by the cave air circulation, E_{rock} is the conduction by ground thermal heat, ΔE_{water} is the sensible and latent heat by liquid water influxes, LE_{air} is the latent heat if there is snow intrusion into the cave and R is the net solar radiation. On the right side, ΔSE_{ice} represents the sensible heat stored in the accumulated ice and ΔLE_{ice} is the latent heat in the ice body, that represents the ice mass changes as well. If $\Delta SE_{ice} + \Delta LE_{ice} > 0$, the mass and energy balance of the ice is negative.

The heat advection due to air circulation can be calculated with the following formula:

$$\Delta E_{air} = \int_{\text{time}} Q_{air} \times \Delta h_s \times dt \quad (\text{J}) \quad (6.4)$$

where ΔE_{air} is the energy change in the system caused by the air currents, Q_{air} is the mass flow rate of dry air in $kg.s^{-1}$ and Δh_s represents the specific enthalpy of humid air exchanged at the boundaries in $J.kg^{-1}$ (Luetscher & Jeannin, 2004b).

Providing that the difference between the cave wall temperature and the system boundaries remain constant on an annual average, the following equation can be used to describe the conductive heat exchanges:

$$E_{rock} = \int_{1 \text{ year}} \varphi \times S_{wall} \times dt \quad (\text{J}) \quad (6.5)$$

where ΔE_{rock} is the energy provided by the ground heat in J , the φ represents the ground heat flux in $W.m^{-2}$, while the S_{wall} is the surface area where the exchange takes place. The ground heat flux is usually measured between 1 and $1.5 W.m^{-2}$ in a limestone cave, presuming a heat conductivity of $2.2 W.m^{-1}.K^{-1}$ and constant conditions.

Intruding seepage water has a significant effect on the cave energy balance. Water has a high thermal capacity ($4180 J.kg^{-1}.K^{-1}$) compared to the limestone. In the *homothermic phreatic zone* of the cave, where the pores are fully saturated, the limestone has an annual average temperature close to the infiltrating water temperature ($T_{rock} = T_{infiltratingwater}$).

$$\Delta E_{water} = c_w \int_{1 \text{ year}} Q_m \times T \times dt \quad (\text{J}) \quad (6.6)$$

where E_{water} is the energy advected by the water fluxes in J , c_w is the heat capacity of water in $J.kg^{-1}.K^{-1}$, Q_m is the mass flow rate of water in $kg.s^{-1}$ and T is the water temperature in K .

In case of certain caves, snow can intrude in direct precipitation form. Damp snow has a density of $150 \pm 50 kg.m^{-3}$ and a latent heat value of $3.35 \times 10^5 J.kg^{-1}$, depending on the position and size of cave entrances, it can significantly contribute to the thermal budget of the system.

Direct solar radiation is also very rare in cave environments, which can nurture perennial ice in non-permafrost regions.

Luetscher et al. (2008) concluded in his findings that the *Monlesi* cave lost $90 \pm 14 m^3$ ice volume in the 2002-2003 observation period. It can be translated to an energy of $28 \pm 5 GJ$ that was gained in that given timeframe. He reported the following measurements:

$$\begin{aligned}
& \Delta E_{air}(-75 \pm 8) + E_{rock}(126 \pm 25) \\
& + \Delta E_{water}(4.4 \pm 0.6) + LE_{snow}(-10.6 \pm 0.6) + R(0) \\
& = \Delta SE_{ice}(0) + \Delta LE_{ice}(28 \pm 5)
\end{aligned} \tag{6.7}$$

According to the interpretation of Luetscher et al. (2005) the energy balance of a cave system is largely dominated by the conductive heat fluxes of the rock in the homothermic phreatic zone (see Fig. 2.2). In other sections of the cave, where a *heterothermic vadose* (unsaturated) regime could be observed, forced air convection would be the defining factor regarding the thermal budget. The reason why ice can accumulate in altitudes where the outside annual mean air temperature is above 0°C can probably be attributed to this fact.

The first systematic study of the *Fuji* ice cave was carried out by Ohata et al. (1994). It is considered to be one of the first comprehensive thermal budget models of an ice cave. He outlines the concept that was decades later used by Luetscher et al. (2003) in the case of the *Monlesi*, while Schöner et al. (2011) and Obleitner and Spötl (2011) at the *Eisriesenwelt*. The sensible and latent heat exchanges were derived from the following equations:

$$SH = a \times \rho \times C_{air} \times U_E \times (T_{inflow} - T_{cave}) \times d \times A_{entrance} \tag{6.8}$$

where SH is the sensible heat energy, a is a correctional coefficient, C_{air} is the specific heat of air, U_E is the air flow velocity at the entrance, T_{inflow} is the inflowing air temperature, T_{cave} is the mean air temperature of the cave, d is the duration, while $A_{entrance}$ represents the surface area of the entrance.

$$LH = \rho \times L_{vapor} \times U_E \times (s_{inflow} - s_{cave}) \times d \times A_{entrance} \tag{6.9}$$

where L_{vapor} is the latent heat of water vapor, U_E is the air flow velocity at the entrance, s_{inflow} is the inflowing specific air humidity, s_{cave} is the specific humidity of the cave air.

Converting the calculations (in GJ) from the *Fuji* cave (Ohata et al., 1994) and from the *Monlesi* cave (Luetscher et al., 2008) to energy fluxes ($W.m^{-2}$), the results share a number of similarities with the findings of Obleitner and Spötl (2011) in the *Eisriesenwelt*.

1. *Eisriesenwelt*, Austria

- SHF = -0.16 W.m^{-2}
- LHF = -0.17 W.m^{-2}
- GHF = 0.07 W.m^{-2}
- NR = 1.00 W.m^{-2}

2. *Fuji* cave, Japan

- SHF = -1.6 W.m^{-2}
- LHF = -0.8 W.m^{-2}
- GHF+NR+PHF = 2.0 W.m^{-2}

3. *Monlesi* cave, Switzerland

- SHF = -0.5 W.m^{-2}
- LHF = -0.4 W.m^{-2}
- GHF+NR = 1.0 W.m^{-2}

6.3 Cave airflow models

Badino (2010) points out that the thermal fluxes conducted by air circulation are highly overestimated compared to the energy input due to seepage water influx. Although it is in contrast to the findings of Luetscher et al. (2008), the air circulation could be influenced at a reasonable cost, whereas it can not be said about the water inflows. Therefore it is in the interest of the cave management to focus the study on the air influxes.

Ice caves can be classified as static and dynamic depending on their ventilation type. The static caves function similar to cold air traps which usually have only one entrance. They have a closed and an open phase. During the summer, the cave has a lower temperature than the outside atmosphere and therefore almost no air influx occurs due to gravitational air mass transport; the cave is in the closed phase. The inside cave temperature has a vertical gradient parallel to the specific weight of the air masses. The less dense warmer air rises to the upper part of the cave, while the denser and colder air sinks to the bottom. In the winter season, when the outside temperatures are lower, the cave has a different airflow regime. Its temperature and air flows correlate more with the outside climatic conditions. This is the period when the cave cools down due to the incoming lower air temperature (Meyer et al., 2015).

Dynamic caves require a more complex approach. These caves have multiple entrances at different heights. The air flows are induced by multiple factors, but generally are related to the temperature (convective circulation) and pressure gradient (barometric circulation) differences. Barometric circulation is induced by the variability of air pressure. In dynamic caves, with entrances at different altitudes and relatively small entrance area/cave volume ratio, this process is not as large in magnitude as the convective circulation.

Badino (2018) argues that the convective circulation has two additional, but mostly hidden causes: “barometric changes induced by variations in the outside temperature and airflow due to anomalous (non-neutral equilibrium) external atmospheric lapse rates”.

In the winter regime, the air at the lower entrance of the dynamic caves is colder. It is due to the fact that the intruding air masses are warmed up by the cave interior walls, escaping through the entrances at a higher altitude, whereas the denser and colder air is sucked into the cave at lower altitudes. This period is characterized by high air velocity values at the cave entrances (Williams & McKay, 2015).

In the *Dachstein-Rieseneishöhle* the *chimney effect* has the largest influence on the air circulation rate. It is notably visible in the clear heterothermic zones, such as the *Tristandom* (See Fig. 6.2). Bock et al. (1913) argues, that the airflow velocity in a dynamic cave is a function of the temperature and the entrance altitude differences:

$$\nu = \mu \sqrt{2gH \frac{T_a T_c}{273 + T_c}} \quad (6.10)$$

where ν is the airflow velocity, μ is a coefficient, which represents the cave geometry, H is the altitude difference between the cave entrances, T_a is the outside temperature, while T_c is the cave temperature.

In his analysis of the *Fuji* cave in Japan, Ohata et al. (1994) shows that there is a proportionality between the airflow velocity and the square root of the temperature differences, when the outside temperature is higher than the cave temperature ($T_{cave} - T_{outside} > 0$):

$$\nu = c \sqrt{|T_{cave} - T_{outside}|} \quad (6.11)$$

where c is a coefficient, which represents the cave geometry, such as the μ by Bock. The analysis of the velocity values in the DRE revealed that the summer regime correlates ($\nu = 0.09\sqrt{\Delta T} + 0.014$, $R^2 = 0.64$) to the findings of Ohata. The velocity values during the winter phase are in the higher range ($1.5 - 2.5 \text{ m.s}^{-1}$), while the

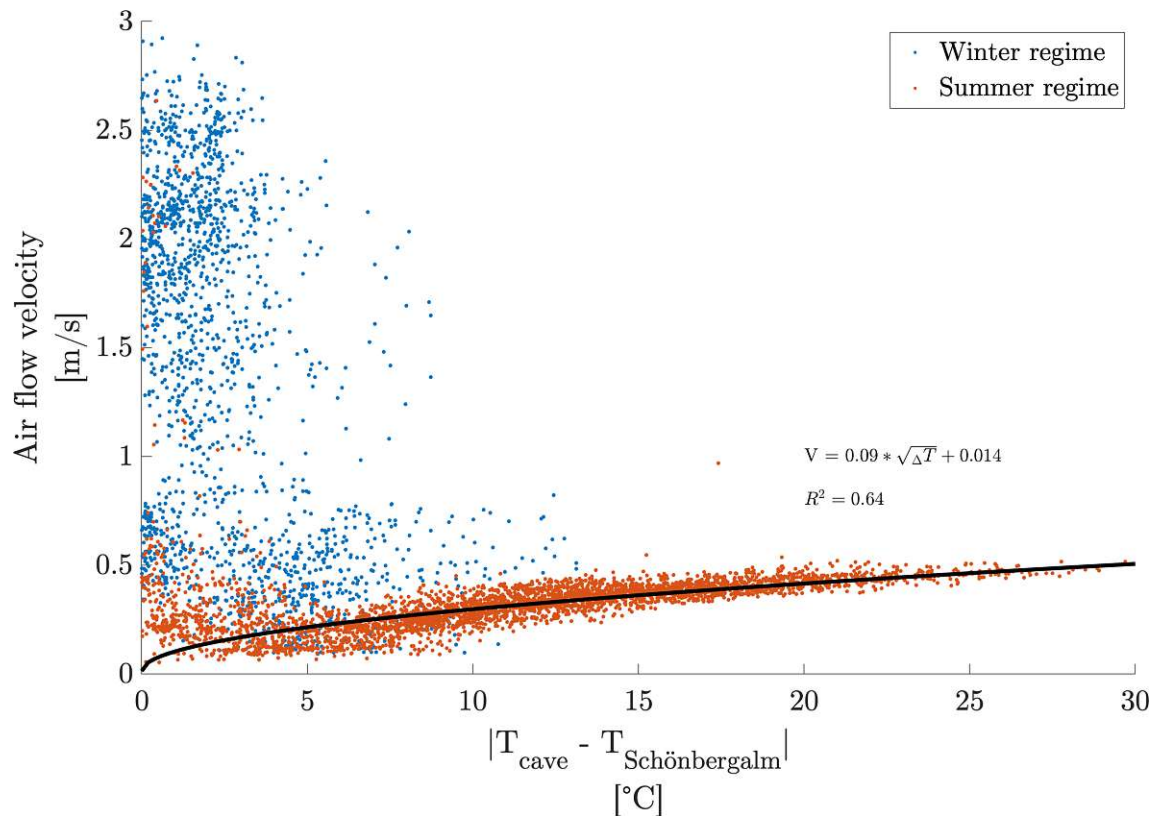
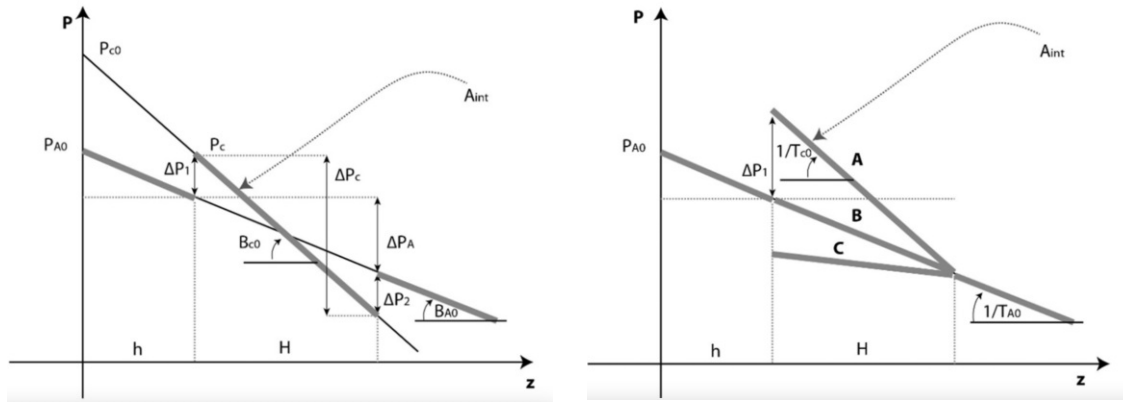


Figure 6.2: Air flow velocity compared to the the outside and cave temperature difference in the *Tristandom*. The measurement points illustrate hourly values from the whole 2019 year. There should be a proportionality between the air velocity and the square root of ΔT .

temperature differences remain lower on average ($0 - 4\text{ }^{\circ}\text{C}$) than in the summer months. Ohata mentions a similar change; when $T_{cave} - T_{outside} < 0\text{ }^{\circ}\text{C}$, then the velocity measurements are close to constant.

Critical temperature

Cave air circulation anomalies have already been reported since the early twenties. In these cases the airflow directions do not match with the actual cave regime due to an unexpected outside temperature. Saar (1953) called it “critical temperature”. He suggests that there is a temperature range around the annual average temperature, where the circulation regime follows a pattern associated with a different astronomical season. In his findings, Saar puts this range in the DRE between 0 and $6\text{ }^{\circ}\text{C}$ ($T_{outside}$), where the summer air circulation regime reaches a turning point and the convective airflow is reversed; outside air masses start to flow into the cave. Given that the air flow rate should be proportional to the difference of temperature gradients (as Eq. 6.10 and 6.11 would suggest), Fig. 6.2 indicates some additional variables.



(a) Explanation of the outside and cave pressure gradient differences.

(b) Pressure gradients at the different seasons. A - summer, C - winter.

Figure 6.3: Notes. Reprinted from “Models of temperature, entropy production and convective airflow in caves”, Badino, 2018, p. 15.

In an attempt to model the cave air circulations, using the hydrostatic equation is a common approach. The method of comparing the outside air column to the cave air column was already used by Bock et al. (1913). The altitude difference between the cave entrances, H and the difference between the air densities (outside and inside the cave), $\Delta\rho$ induce the pressure difference at the cave inlets, ΔP . Badino (2010) calls it the “moving pressure” (or later the “driving pressure”), and proposes the following formula:

$$\Delta P = \rho_{cave} \times \left(\frac{\Delta T}{T_{ext}} \right) \times g \times H \quad (6.12)$$

where ΔP is the moving pressure, ρ_{cave} is the average cave air density, ΔT is the average air temperature difference between the outside (T_{ext}) and cave atmosphere, while H represents the cave altitude differences.

In his study of the *Eisriesenwelt*, Thaler (2008) suggests a model that is built on the hydrostatic pressure equation and the temperature gradients. He calls the point, where the outside and cave pressure is in equilibrium, “*Gleichgewichtstemperatur*”. He calculates the outside and the cave air column pressures using the *virtual temperature*. It is a method utilized often in meteorology, where the temperature value contains information about the relative humidity of the air mass:

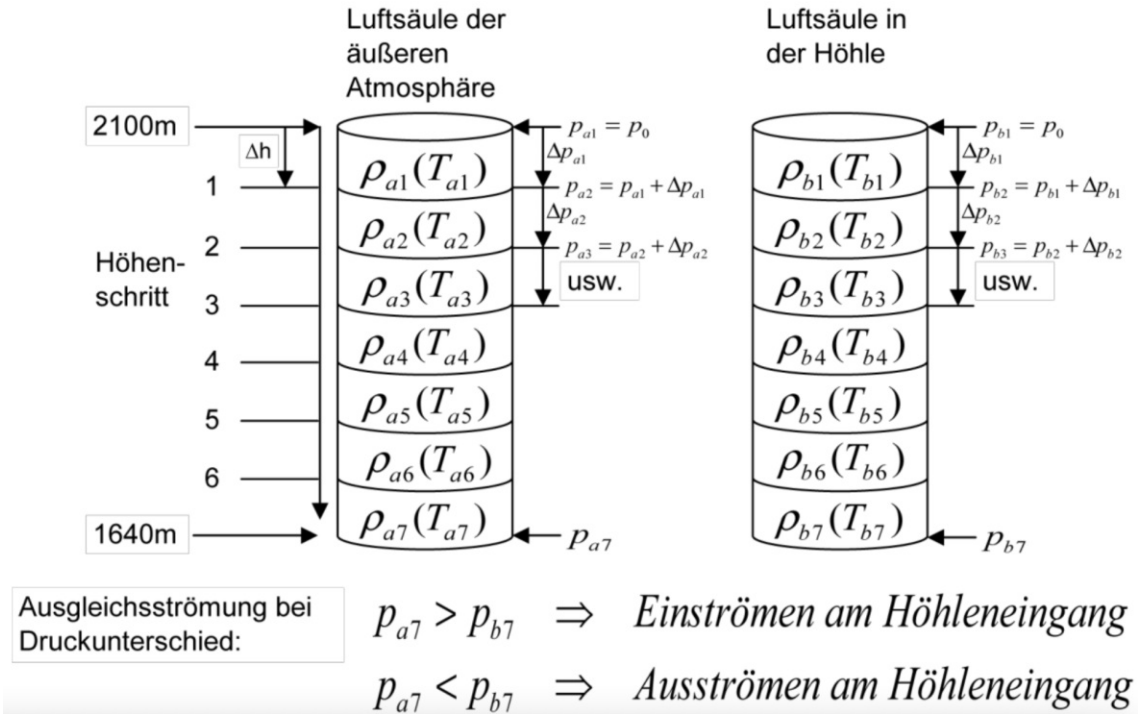


Figure 6.4: Hydrostatic pressure model used by Thaler in the *Eisriesenwelt*. If the pressure of the inside air column is bigger than that of the outside air column, then the air starts to flow outwards. *Notes.* Reprinted from “Analyse der Temperaturverhältnisse in der Eisriesenwelt-Höhle im Tennengebirge anhand einer 12 jährigen Messreihe”, Thaler, 2008, p. 51.

$$T_{virtual} = T \left(1 + \frac{1}{f e_s(T) \left(1 - \underbrace{\frac{R_L}{R_W}}_{\approx 0,378} \right) - 1} \right) \approx T \left(1 + \frac{1}{\frac{p}{0,378 f e_s(T)} - 1} \right) \quad (6.13)$$

where $T_{virtual}$ is the virtual temperature, f is the relative humidity and $e_s(T)$ is the saturation vapor pressure.

The difference between T and $T_{virtual}$ rises as the air is becoming more saturated (see Fig. 7.2 and 7.3). He provides the following formula to determine the pressure of the air columns (see Fig. 6.4):

$$p_i = p_{i-1} + \Delta p_i = p_{i-1} - \frac{g}{R_L} \frac{p_{i-1}}{T_{virtual}(h_i)} \Delta h \quad (6.14)$$

where p_i is the pressure at the given altitude (he modeled the temperature gradients in 10 m steps), Δh is the altitude step, h_i is the altitude, p_{i-1} is the pressure at the previous altitude step and $T_{virtual}$ is the temperature calculated with the Eq. 6.13.

Badino (2018) claims that the barometric circulations indicated by the temperature differences (he established the term *thermal barometric circulation*) have a much larger impact in lower altitudes ($H < 1000\text{ m}$). It has consequences in the daily circulations changes, when the daily temperature variation is significant. Furthermore, the notion that the driving pressure of the convective airflows is zero, when the outside and the cave temperature are close to equal, has been demonstrated to be false. He recommends the usage of the *neutral temperature of convection*, as an improvement of the hydrostatic approach.

$$X_A(h) = T_c + \frac{1}{2} \times (G_A - G_c) \times H \quad (6.15)$$

where $X_A(h)$ is the temperature at altitude h (cave lower entrance), where the driving pressure is zero, T_c is the cave temperature in $^{\circ}\text{C}$, G_A is the general external lapse rate (temperature gradient) in $^{\circ}\text{C.km}^{-1}$, G_c is the cave lapse rate (temperature gradient) in $^{\circ}\text{C.km}^{-1}$, while H is the altitude difference between the cave entrances in km .

Equation 6.15 indicates that the air circulation stops, when the outside air temperature at the lower entrance comes close to the inside cave temperature with a correction factor (given that the outside and the cave lapse rate between the lower and the upper entrance are constant). This factor is composed of the lapse rate differences and the height of the cave.

In Badinos approximation that was validated in the *Su Bentu* cave in Sardinia, in summer $T_c + 0.25H < X_A(h) < T_c + 1.25H$, whereas during the winter months $T_c - 8.25H < X_A(h) < T_c + 1.75H$.

Chapter 7

Conclusion and Outlook

The ongoing microclimate monitoring effort of the *Dachstein-Rieseneishöhle* offers a paramount opportunity for the cave management to benefit from these observations. In order to preserve this unique climatic archive, the detrimental effects of the warming climate should be negated as much as possible.

Temperature change rates of the *Dachstein* region in the past decades predict a continuous rise in the mean annual values. This affects not only the thermal heat influx by the air exchange between the inner parts of the cave and the outside climate, but also raises the temperature of precipitation penetrating the karst, which mostly dictates the thermal budget of the homothermic zone.

The historical comparison confirms the findings of multiple scientists who studied climate change in the Alps. It provides a good enough correlation throughout the past years that a significant deceleration of the local temperature increases should not to be expected.

The dominance of the various thermal energy influxes (seepage water and air circulation) in the unsaturated cave zone might be argued between experts, but the trends regarding the outside temperatures notably drift to one direction. This energy surplus works against the ice accumulation of non-permafrost caves in the long haul.

To maximize accumulation opportunities, the different glaciation periods must be investigated separately as well. A shortened cooling and an elongated melting period should be anticipated, whereas a greater variation in the freezing period's length and precipitation volume should be considered. Although the overall energy balance will be affected by the higher water temperature (it tends to reflect the annual air temperature in the region), the freezing period should still be harnessed to its fullest potential.

It is not plausible to considerably limit the water inflow, but it is feasible to block (already utilized in the DRE and in many other caves) or to increase air exchange between the outside and the cave. Besides weather doors, mechanical ventilation could function as a supplementary means actively increasing the cold winter air intake. Especially helping the halls in the heterothermic zone where the outer climate has a bigger impact on the glaciation rate. The *Tristandom's* proximity to the exit presents a great opportunity during the winter months. Endowed with the ability to increase the airflow - even when the outside climate reaches the critical temperature, although it is still cooler than the cave - would help to lessen the annual warming effects inside the cave and utilize the cooling period more efficiently.

However, given the scale of the warming, caution must be exercised regarding the possible effects of the aforementioned interventions. There is only limited data available from caves with similar apparatus. Obleitner and Spötl (2011) estimates that in the case of the *Eisriesenwelt*, operating a weather door might save around 5 mm.y^{-1} ice, which is one order of magnitude smaller than the annual retreat.

7.1 Future research

Looking forward, it is important to maintain a long-term and high-quality observation program focusing on the cave microclimate. The outer climate is already well monitored by the two nearby stations. An ongoing multi-year effort would eliminate noise and errors from the dataset and would provide an ever growing data-pool that could be used by statistical models that could help validate physical models.

Future research should be devoted to establish an automated schedule for the available and potential mechanical aids (doors and/or ventilation). This could be based on the physical models such as Eq. 6.14 of Thaler or Eq. 6.15 of Badino, complemented with the actual air flow velocity and direction measurements, which might validate or contradict a potential prediction.

The possibility of using a statistical model for scheduling purposes warrants further investigation. An adequate solution could be a recurrent neural network with inputs based on the physical models (outside temperature gradient, cave temperature and airflow vectors). The data is a continuous time series consisting of values whose relations are based in thermodynamics. There is a good probability that these models could be trained to achieve better results than the hydrostatic-based ones, since the complex cave environments require a significant amount of conjecture.

Regarding the ice mass, continuous ice thickness measurements (i.e. with an ultrasonic ranger) could play a pivotal role in validating mass and energy balance models, as well as a thermal radiation sensor in the homothermic zone that might corroborate the observations from the neighboring *Eisriesenwelt* (Obleitner & Spötl, 2011; Schöner et al., 2011) . Ice temperature measurements have already been started, although they were hindered by instrument malfunctions. Additional data collection could include the dripping water rate which could be then approximated to indicate the thermal impact of the water influx in the energy balance and vertical

Bibliography

- Badino, G. (2018). Models of temperature, entropy production and convective airflow in caves. *Geological Society, London, Special Publications*, 466.
- Badino, G. (2010). Underground meteorology- what's the weather underground? *Acta Carsologica*, 39(3).
- Balch, E. S. (1900). *Glacières or freezing caverns*. Allen, Lane Scott.
- Bock, H., Lahner, G., Gaunersdorfer, G., & für Höhlenkunde in Österreich., V. (1913). *Höhlen im dachstein und ihre bedeutung für die geologie, karsthydrographie und die theorien über die entstehung des höhleneises*. Im Verlage des Vereines für Hohlenkunde in Österreich, Deutsche Vereins-Druckerei Graz.
- Fairchild, I. J., Baker, A., Asrat, A., Dominguez-Villar, D., Gunn, J., Hartland, A., & Lowe, D. (2012). *Speleothem science: From process to past environments*. Wiley-Blackwell.
- Fairchild, I. J., Baker, A., Fuller, L., Borsato, A., Miorandi, R., Frisia, S., Matthey, D., McMillan, E., Spötl, C., & Andreo, B. (2006). Speleophysiology: A key to understanding high-resolution information in speleothems. *Archives of Climate Change in Karst: Proceedings of the Symposium: Climate Change the Karst Record, IV. Karst Waters Institute Special Publication*, 10, 249.
- Fugger, E. (1891). *Eishöhlen und windröhren*. Separat-Abdruck XXIV. Jahresberichte der K.K. Ober-Realschule in Salzburg.
- Fugger, E. (1893). *Eishöhlen und windröhren. dritter theil (schluss)*. Separat-Abdruck XXVI. Jahresberichte der K.K. Ober-Realschule in Salzburg.
- Gobiet, A., Kotlarski, S., Beniston, M., Heinrich, G., Rajczak, J., & Stoffel, M. (2014). 21st century climate change in the european alps - a review. *Science of The Total Environment*, 493, 1138–1151.
- Holzmann, H., & Koboltschnig, G. (2010). Hydrologische veränderungen in hochalpinen einzugsgebieten. *Auswirkungen des Klimawandels auf Hydrologie und Wasserwirtschaft in Österreich*, 61–71.

- Jordan, R. (1991). *A one-dimensional temperature model for a snow cover : Technical documentation for sntherm.89* (tech. rep. No. 91-16). U.S. Army Cold Regions Research and Engineering Laboratory.
- Karakostanoglou, I. (1989). Some remarks on the genesis and geography of static ice shafts. In T. Hazslinszky & K. Takácsné Bolner (Eds.), *Proceedings* (pp. 713–715). Hungarian Speleological Society.
- Luetscher, M., & Jeannin, P. Y. (2004a). A process-based classification of alpine ice caves. *Theoretical and Applied Karstology*, *17*, 5–10.
- Luetscher, M., & Jeannin, P. Y. (2004b). The role of winter air circulations for the presence of subsurface ice accumulations: An example from monlési ice cave (switzerland). *Theoretical and Applied Karstology*, *17*, 19–25.
- Luetscher, M., & Jeannin, P. Y. (2004c). Temperature distribution in karst systems: The role of air and water fluxes. *Terra Nova*, *16*(6), 344–350.
- Luetscher, M., Jeannin, P. Y., & Haeberli, W. (2003). Energy fluxes in an ice cave of sporadic permafrost in the swiss jura mountains—concept and first observational results. *Permafrost, Proceedings, Eighth International Conference on Permafrost*, *21*.
- Luetscher, M., Jeannin, P. Y., & Haeberli, W. (2005). Ice caves as an indicator of winter climate evolution: A case study from the jura mountains. *The Holocene*, *15*(7), 982–993.
- Luetscher, M., Lismonde, B., & Jeannin, P. Y. (2008). Heat exchanges in the heterothermic zone of a karst system: Monlesi cave, swiss jura mountains. *J. Geophys. Res.*, *113*.
- Malyudov, B. (1989). Cave glaciation. In T. Hazslinszky & K. Takácsné Bolner (Eds.), *Proceedings* (pp. 298–300). Hungarian Speleological Society.
- Meyer, C. (2018). Chapter 2 - history of ice caves research. In A. Perşoiu & S.-E. Lauritzen (Eds.), *Ice caves* (pp. 5–20). Elsevier.
- Meyer, C., Meyer, U., Pflitsch, A., & Maggi, V. (2015). Analyzing airflow in static ice caves by using the calcflo method. *The Cryosphere Discussions*, *9*, 5291–5326.
- Meyer, C., Pflitsch, A., Ringeis, J., & Maggi, V. (2017). Reports on ice caves in literature from the twelfth to the middle of the twentieth century. *Journal of cave and karst studies*, *79*(3), 141–145.
- Obleitner, F., & Spötl, C. (2011). The mass and energy balance of ice within the eisriesenwelt cave, austria. *The Cryosphere*, *5*(1), 245–257.
- Ohata, T., Furukawa, T., & Higuchi, K. (1994). Glacioclimatological study of perennial ice in the fuji ice cave, japan. part 1. seasonal variation and mechanism of maintenance. *Arctic and Alpine Research*, *26*(3), 227–237.

- Saar, R. (1953). Beiträge zur meteorologie der dynamischen wetterhöhlen. *Mitteilungen der höhlenkommission beim bundesministerium für land- und forstwirtschaft* (pp. 4–52).
- Saar, R. (1954). Meteorologisch-physikalische beobachtungen in der dachstein-hieseneishöhle. *Die Höhle*, 5, 49–62.
- Saar, R. (1955). Die dachstein-rieseneishöhle nächst obertraun und ihre funktion als dynamische wetterhöhle. *Jahrbuch des oberösterreichischen musealvereines* (pp. 263–319).
- Saar, R. (1957). Zur frage des einflusses der grosswetterlage auf die dynamik der wetterhöhlen. *Die Höhle*, 8, 33–44.
- Schmeidl, H. (1969). Zur pollenanalytischen altersbestimmung der eisbildungen in der schellenberger eishöhle und in der dachstein-rieseneishöhle. *Jahrbuch des vereins zum schutze der alpenpflanzen und -tiere* (pp. 67–84).
- Schöner, W., Weys, G., & Mursch-Radlgruber, E. (2011). Linkage of cave-ice changes to weather patterns inside and outside the cave eisriesenwelt. *The Cryosphere*, 5(3), 603.
- Stummer, G. (1999). Die speläokartographische darstellung der dachstein-rieseneishöhle im wandel der zeit. *Die Höhle*, 50(3), 141–147.
- Thaler, K. (2008). *Analyse der temperaturverhältnisse in der eisriesenwelt-höhle im tennengebirge anhand einer 12 jährigen messreihe* (Master's thesis). Leopold-Franzens Universität.
- Turri, S., Trofimova, E., Bini, A., & Maggi, V. (2009). Ice caves scientific research history; from xv to xix centuries. *Materialy Glyatsiologicheskikh Issledovaniy*, 107, 156–162.
- Wigley, T. M. L., & Brown, C. (1971). Geophysical applications of heat and mass transfer in turbulent pipe flow. *Boundary-Layer Meteorology*, 1(3), 300–320.
- Williams, K., & McKay, C. (2015). Comparing flow-through and static ice cave models for shoshone ice cave. *International Journal of Speleology*, 44.

Appendix

Table 7.1: Rock temperature measurements by Saar in 1928-29.

T			<i>Eingangsstollen</i>		<i>Belrapeire</i>		
			50 cm	100 cm	50 cm	100 cm	150 cm
1928	Dec	20	-4,3	-2	-	-	-
1928	Dec	28	-	-	-2,4	-2	-1,7
1928	Dec	29	-	-	-2,9	-1,6	-1,3
1929	Jan	4	-5	-2	-	-	-
1929	Jan	5	-	-	-3,2	-2,1	-1,9
1929	Jan	30	-5,4	-4	-	-	-
1929	Jan	31	-	-	-5,3	-4,2	-3,7
1929	Feb	14	-12,5	-6,1	-9,5	-5,9	-5,3
1929	Feb	15	-12,2	-6,8	-	-	-
1929	Feb	16	-10,7	-6,1	-	-	-
1929	Mar	2	-7	-4	-6,9	-5,9	-5,5
1929	Mar	3	-6,6	-4,5	-	-	-
1929	Mar	11	-	-	-5,4	-5,5	-5,5
1929	Mar	18	-2,1	-2,5	-	-	-
1929	Apr	3	-	-	-3	-3	-3
1929	Apr	13	-2	-2	-	-	-
1929	Apr	17	-1,7	-1,7	-2,7	-3	-3,2
1929	May	7	-0,6	-1	-2	-2,2	-2,5
1929	May	19	-	-	-1,5	-1,7	-2,1
1929	Jun	9	0	-0,4	-	-	-
1929	Jun	10	-	-	-1,3	-1,4	-1,6
1929	Jun	27	0	-0,2	-1,3	-1,1	-1,5
1929	Jul	12	-0,2	-0,2	-1	-1	-1,2
1929	Jul	26	0	-0,1	-0,9	-0,9	-0,9
1929	Aug	5	0	-0,1	-0,8	-0,8	-1
1929	Aug	19	0	-0,1	-0,7	-0,7	-1
1929	Sep	4	0	-0,1	-0,5	-0,5	-0,7
1929	Sep	15	0	-0,1	-0,5	-0,5	-0,7
1929	Oct	1	-	-	-0,5	-0,5	-0,6
1929	Oct	2	0	0	-	-	-

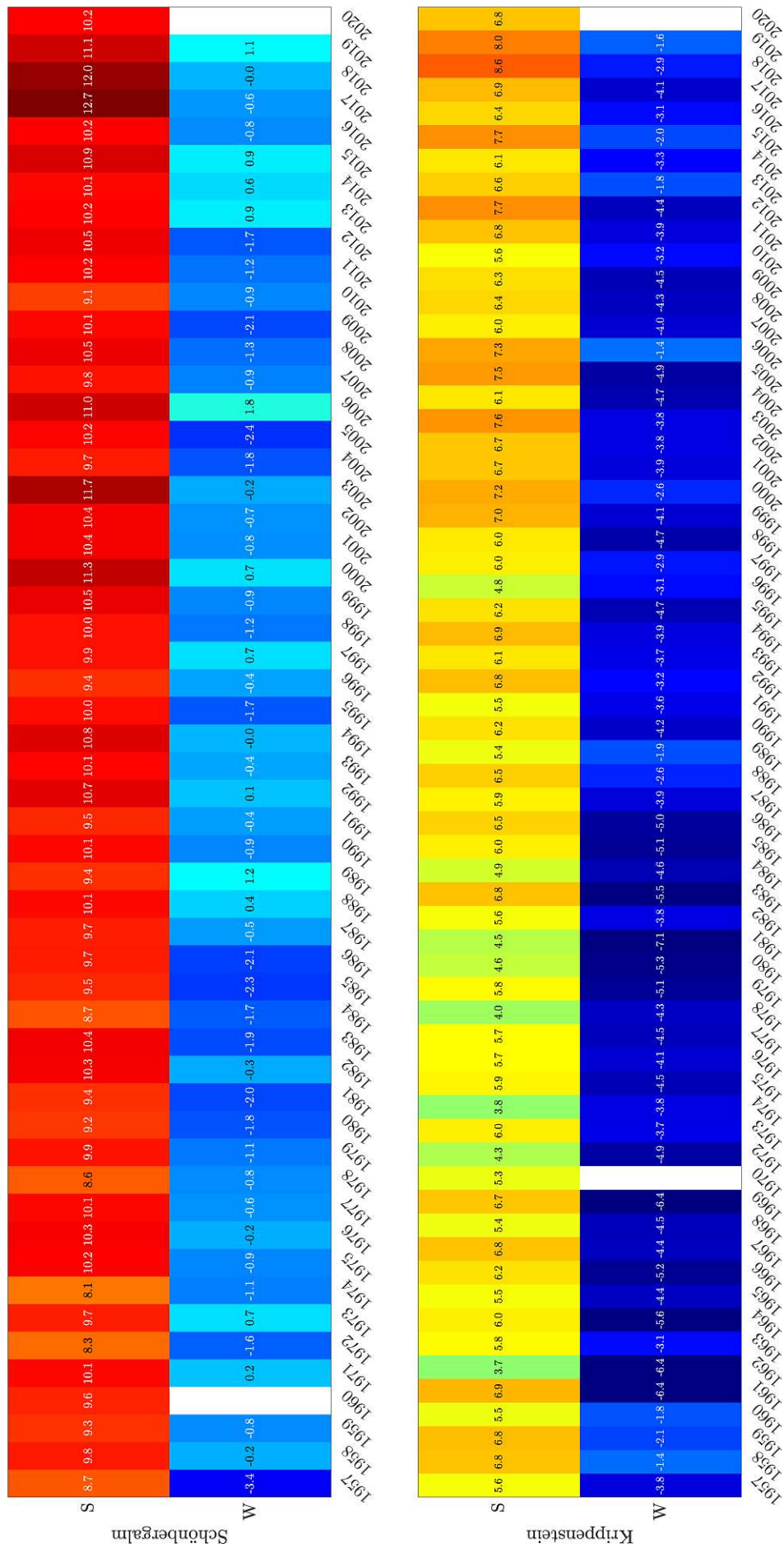


Figure 7.3: Heatmap of Schönbergalm and Krippenstein grouped by the summer and winter regimes

Table 7.2: $\Delta T = T_{\text{measurement}} - T_{\text{virtual}}$ at different temperatures and relative humidity levels.

ΔT [°C]	T [°C]															
	-10	-8	-6	-4	-2	0	2	4	6	8	10	12	14	16	18	20
0	0,00	0,00	0,00	0,00	0,00	0,00	0,00	0,00	0,00	0,00	0,00	0,00	0,00	0,00	0,00	0,00
5	0,02	0,04	0,04	0,04	0,04	0,04	0,04	0,04	0,05	0,06	0,07	0,06	0,06	0,07	0,08	0,12
10	0,04	0,05	0,06	0,06	0,07	0,07	0,08	0,09	0,10	0,10	0,12	0,13	0,14	0,15	0,17	0,20
15	0,05	0,07	0,08	0,08	0,09	0,10	0,11	0,13	0,15	0,17	0,19	0,22	0,24	0,28	0,32	0,38
20	0,06	0,08	0,09	0,10	0,11	0,12	0,14	0,17	0,20	0,23	0,26	0,30	0,34	0,39	0,45	0,52
25	0,07	0,09	0,11	0,12	0,14	0,15	0,18	0,21	0,24	0,28	0,33	0,37	0,43	0,49	0,57	0,65
30	0,08	0,11	0,13	0,15	0,16	0,19	0,21	0,25	0,29	0,34	0,39	0,45	0,52	0,60	0,69	0,78
35	0,10	0,12	0,15	0,17	0,19	0,22	0,25	0,29	0,34	0,39	0,45	0,53	0,61	0,71	0,80	0,91
40	0,11	0,14	0,17	0,19	0,22	0,25	0,29	0,33	0,38	0,45	0,52	0,61	0,70	0,81	0,92	1,04
45	0,13	0,16	0,19	0,21	0,25	0,28	0,32	0,37	0,43	0,50	0,59	0,68	0,80	0,92	1,04	1,17
50	0,14	0,17	0,21	0,24	0,27	0,31	0,36	0,41	0,48	0,56	0,65	0,76	0,89	1,02	1,16	1,30
55	0,15	0,19	0,23	0,26	0,30	0,34	0,39	0,45	0,52	0,61	0,72	0,84	0,98	1,13	1,28	1,43
60	0,17	0,21	0,24	0,28	0,33	0,37	0,43	0,49	0,57	0,67	0,78	0,92	1,07	1,23	1,40	1,56
65	0,18	0,22	0,26	0,31	0,35	0,40	0,46	0,53	0,62	0,72	0,85	1,00	1,16	1,34	1,51	1,69
70	0,20	0,24	0,28	0,33	0,38	0,44	0,50	0,57	0,67	0,78	0,91	1,08	1,25	1,44	1,63	1,82
75	0,21	0,26	0,30	0,35	0,41	0,47	0,54	0,61	0,71	0,83	0,98	1,15	1,35	1,55	1,75	1,95
80	0,23	0,27	0,32	0,37	0,43	0,50	0,57	0,65	0,76	0,88	1,04	1,23	1,44	1,66	1,88	2,08
85	0,23	0,28	0,33	0,39	0,45	0,52	0,60	0,69	0,80	0,94	1,10	1,31	1,53	1,77	2,00	2,22
90	0,24	0,30	0,35	0,41	0,47	0,55	0,63	0,73	0,85	0,99	1,17	1,38	1,62	1,88	2,13	2,35
95	0,26	0,31	0,37	0,43	0,50	0,58	0,67	0,78	0,90	1,05	1,23	1,46	1,72	1,98	2,25	2,49
100	0,28	0,34	0,40	0,47	0,54	0,62	0,72	0,83	0,96	1,12	1,30	1,54	1,81	2,09	2,36	2,61

 RH
 [%]

Table 7.3: $T_{virtual}$ at different temperatures and relative humidity levels.

$T_{virtual}$ [°C]	T [°C]															
	-10	-8	-6	-4	-2	0	2	4	6	8	10	12	14	16	18	20
0	-10,00	-8,00	-6,00	-4,00	-2,00	0,00	2,00	4,00	6,00	8,00	10,00	12,00	14,00	16,00	18,00	20,00
5	-9,98	-7,96	-5,96	-3,96	-1,96	0,04	2,04	4,04	6,05	8,06	10,07	12,06	14,06	16,07	18,08	20,12
10	-9,96	-7,95	-5,94	-3,94	-1,93	0,07	2,08	4,09	6,10	8,12	10,13	12,14	14,15	16,17	18,20	20,25
15	-9,95	-7,93	-5,92	-3,92	-1,91	0,10	2,11	4,13	6,15	8,17	10,19	12,22	14,24	16,28	18,32	20,38
20	-9,94	-7,92	-5,91	-3,90	-1,89	0,12	2,14	4,17	6,20	8,23	10,26	12,30	14,34	16,39	18,45	20,52
25	-9,93	-7,91	-5,89	-3,88	-1,86	0,15	2,18	4,21	6,24	8,28	10,33	12,37	14,43	16,49	18,57	20,65
30	-9,92	-7,89	-5,87	-3,85	-1,84	0,19	2,21	4,25	6,29	8,34	10,39	12,45	14,52	16,60	18,69	20,78
35	-9,90	-7,88	-5,85	-3,83	-1,81	0,22	2,25	4,29	6,34	8,39	10,45	12,53	14,61	16,71	18,80	20,91
40	-9,89	-7,86	-5,83	-3,81	-1,78	0,25	2,29	4,33	6,38	8,45	10,52	12,61	14,70	16,81	18,92	21,04
45	-9,87	-7,84	-5,81	-3,79	-1,75	0,28	2,32	4,37	6,43	8,50	10,59	12,68	14,80	16,92	19,04	21,17
50	-9,86	-7,83	-5,79	-3,76	-1,73	0,31	2,36	4,41	6,48	8,56	10,65	12,76	14,89	17,02	19,16	21,30
55	-9,85	-7,81	-5,77	-3,74	-1,70	0,34	2,39	4,45	6,52	8,61	10,72	12,84	14,98	17,13	19,28	21,43
60	-9,83	-7,79	-5,76	-3,72	-1,67	0,37	2,43	4,49	6,57	8,67	10,78	12,92	15,07	17,23	19,40	21,56
65	-9,82	-7,78	-5,74	-3,69	-1,65	0,40	2,46	4,53	6,62	8,72	10,85	13,00	15,16	17,34	19,51	21,69
70	-9,80	-7,76	-5,72	-3,67	-1,62	0,44	2,50	4,57	6,67	8,78	10,91	13,08	15,25	17,44	19,63	21,82
75	-9,79	-7,74	-5,70	-3,65	-1,59	0,47	2,54	4,61	6,71	8,83	10,98	13,15	15,35	17,55	19,75	21,95
80	-9,78	-7,73	-5,68	-3,63	-1,57	0,50	2,57	4,65	6,76	8,88	11,04	13,23	15,44	17,66	19,88	22,08
85	-9,77	-7,72	-5,67	-3,61	-1,55	0,52	2,60	4,69	6,80	8,94	11,10	13,31	15,53	17,77	20,00	22,22
90	-9,76	-7,70	-5,65	-3,59	-1,53	0,55	2,63	4,73	6,85	8,99	11,17	13,38	15,62	17,88	20,13	22,35
95	-9,74	-7,69	-5,63	-3,57	-1,50	0,58	2,67	4,78	6,90	9,05	11,23	13,46	15,72	17,98	20,25	22,49
100	-9,72	-7,66	-5,60	-3,53	-1,46	0,62	2,72	4,83	6,96	9,12	11,30	13,54	15,81	18,09	20,36	22,61

 RH
 [%]

Table 7.4: Mean daily temperatures in 1928-29 by Saar.

T		St. I.	St. II.	St. III.	St. IV.	St. V.	St. VI.
		MS 17	MS 16	MS 14	MS 10	MS 9	MS 5
1928	Jul	13,9	0,7	0,9	0	0,1	1,3
1928	Aug	13,4	0,7	0,7	0,7	0,5	1,1
1928	Sep	8,1	0,8	0,6	0,7	0,7	1,1
1928	Oct	6,1	0,6	0,6	0,6	0,6	1
1928	Nov	2	0,2	0,6	0,4	0,7	1
1928	Dec	-3,4	-3,9	-3,6	-2,1	-1,1	0,5
1929	Jan	-5,5	-5,2	-4,7	-5,4	-2,6	0,2
1929	Feb	-8,2	-8,4	-8,4	-7,1	-4,9	-1,9
1929	Mar	-1,1	-5,8	-4,4	-5,7	-3,9	-1,2
1929	Apr	1,4	-3,1	-3,1	-2,7	-2,6	-
1929	May	5,9	-1,6	-2,3	-2,4	-1,7	-
1929	Jun	9,8	-1,4	-1,3	-1,3	-1,1	-
1929	Jul	13,3	-0,4	-0,5	-1,1	-1,3	-
1929	Aug	12,8	-0,7	-0,1	-0,5	-0,5	-
1929	Sep	13,2	-0,4	0	-0,6	-0,4	-

Table 7.5: Daily max and min temperatures in 1928-29 by Saar.

T	St. I.		St. II.		St. III.		St. IV.		St. V.		St. VI.	
	MS 17		MS 16		MS 14		MS 10		MS 9		MS 5	
	Max	Min	Max	Min	Max	Min	Max	Min	Max	Min	Max	Min
1928 Jul	30,2	6,2	1,2	0,4	1,1	0,3	0,9	-0,8	0,5	-0,8	2,2	0,9
1928 Aug	31,5	0,5	1,2	0,4	0,9	0,7	1,1	-0,2	0,5	0,5	1,3	0,9
1928 Sep	28	-2,5	1,4	0,2	1,3	0,3	1,2	0,1	0,9	0,5	1,1	1
1928 Oct	20	-5,2	1,9	0,2	0,9	0,3	0,8	0	1	0,5	1,1	1
1928 Nov	16	-7	1,3	-4,2	1,2	-3,1	1	-1,6	1,3	-0,3	1,1	0,8
1928 Dec	3,5	-11	-2	-8	-1,1	-8	0	-4,3	0	-1,9	0,8	0,3
1929 Jan	-1	-10,3	-3	-13,1	-2,5	-12,7	-3	-8	-1,8	-3,7	0,3	-0,7
1929 Feb	9	-23	-6	-19,5	-3,7	-17,4	-5,4	-9,9	-3,3	-7,5	-1	-2,6
1929 Mar	13	-12	-3	-10	-2,2	-9	-2,8	-8,1	-2,1	-5,6	-1	-1,8
1929 Apr	16	-12,2	-1	-9	-1	-8,2	-2	-4	-2,1	-3,8	-	-
1929 May	23	-2	0,7	-3,4	-0,2	-3,5	-1,5	-3	-1	-2,5	-	-
1929 Jun	27	0,9	-1,1	-2	0	-3,8	-1	-1,9	-0,8	-2	-	-
1929 Jul	32	2	0	-2	0,2	-0,8	-0,8	-1,6	-0,8	-2	-	-
1929 Aug	30	4,1	-0,3	-1	0,5	-0,5	-0,2	-0,9	-0,2	-0,7	-	-
1929 Sep	30	1,8	-0,2	-1,1	0,6	-0,5	-0,4	-1,1	-0,3	-1	-	-

Table 7.6: Daily mean temperature measurements by Saar 1920-22.

Außentemp.		Eiskapelle	Tristandom	Parsivaldom	Artusdom	Plimisoel	Ivanhalle
St. I.	St II.	St. III.	St. IV.	St. VI.	St. 6a	St. 8	St. 8
1920 Aug 10	13,1	1	1,6	1,8	3,2	3	4
1920 Sep 15	7	2	1,7	1,8	3	3,2	4,3
1920 Sep 17	13	1,8	1,4	1,9	3,8	3,3	4,5
1920 Oct 9	7,7	1,3	1,1	1,2	1,7	3,4	4,2
1921 Jun 30	15	0,5	0,5	0,2	2,5	3,2	3,4
1921 Jul 10	14	0,9	0,9	0,4	2,5	2,9	3,5
1921 Sep 5	9	1,2	2,1	1,3	2,5	2,7	3,5
1921 Sep 13	10	1,1	0,8	1,1	2,3	2,9	4,5
1921 Sep 25	10	0,2	0,2	0,4	1,3	-	3,8
1921 Oct 14	8	1,2	1	1,1	1,8	-	3,4
1922 Jan 16	-16	-12	-9	-3,9	0,6	1,5	2
1922 Feb 16	-4,7	-6,2	-5,9	-3,4	0,8	1,3	2,1
1922 Mar 17	-1,7	-3,2	-3,2	-2,5	1,2	1,5	2,6
1922 Apr 25	-0,6	-3,3	-2,4	-2,1	1,2	1,6	2,6
1922 May 14	3,2	-2,2	-1	-1	1,5	2,1	2,7
1922 Jun 18	7,5	-0,5	-0,3	-1,2	1,8	2,3	3
1922 Jul 30	13	-0,9	-0,8	-1	1,9	2,4	2,9
1922 Nov 10	0	-0,3	-0,1	-0,3	1	1,8	2,9
1922 Nov 20	-3	-3,6	-3,5	-0,8	0,8	2	2,7
1922 Dec 1	2	-2,9	-2,6	-1,5	1,2	1,8	2,7
1922 Dec 28	-0,4	-1,9	-1,4	-1,5	1,2	1,9	2,8

Table 7.7: Monthly mean temperatures by Saar from the 1920-24 period.

	Außentemp.		Eiskapelle		Tristandom		Parsivaldom		Artusdom		Plimisoel		Ivanhalle		Wind direction
	St. I.	St. II.	St. III.	St. IV.	St. V.	St. VI.	St. 6a	St. 8							
Jan	-14,7	-10,6	-8,8	-3,4	0,9	1,7	2,1	bergwärts							
Feb	-8,7	-8,3	-6,1	-3,7	0,9	1,3	2,4	bergwärts							
Mar	-0,5	-3,4	-2,4	-2,3	1,2	1,7	2,7	bergwärts							
Apr	0,7	-2,5	-1,4	-1,5	1,4	1,9	2,5	bergwärts							
Mai	10,5	-1,9	-1	-1	1,7	2,2	2,7	wechselnd							
Jun	12,8	-0,2	-0,1	-0,7	1,9	2,7	2,9	talwärts							
Jul	10,8	0,4	0,4	0	2,3	2,5	3,6	talwärts							
Aug	8,6	1,5	2,1	1,5	2,6	2,7	3,6	talwärts							
Sep	10,9	1,1	1,2	1,1	2,3	2,8	3,4	talwärts							
Okt	5,9	1,1	1,3	1,3	1,6	2,7	3,6	wechselnd							
Nov	-2,6	-3,2	-3	-1,3	1,2	1,8	2,9	bergwärts							
Dez	-1,8	-2,5	-2,3	-1,5	1,2	1,9	2,9	bergwärts							
MAAT	2,6	-2,4	-1,7	-0,9	1,6	2,1	2,8								